

Rationalizing the diversity of amide–amide H-bonding in peptides using the natural bond orbital method

Valérie Brenner, Eric Gloaguen, Michel Mons

▶ **To cite this version:**

Valérie Brenner, Eric Gloaguen, Michel Mons. Rationalizing the diversity of amide–amide H-bonding in peptides using the natural bond orbital method. Physical Chemistry Chemical Physics, 2019, 21 (44), pp.24601-24619. 10.1039/c9cp03825f . cea-02370063

HAL Id: cea-02370063

https://cea.hal.science/cea-02370063

Submitted on 26 Nov 2020

HAL is a multi-disciplinary open access archive for the deposit and dissemination of scientific research documents, whether they are published or not. The documents may come from teaching and research institutions in France or abroad, or from public or private research centers.

L'archive ouverte pluridisciplinaire **HAL**, est destinée au dépôt et à la diffusion de documents scientifiques de niveau recherche, publiés ou non, émanant des établissements d'enseignement et de recherche français ou étrangers, des laboratoires publics ou privés.

Rationalizing the diversity of amide-amide H-bonding in peptides using the Natural Bond Orbital method

Valérie Brenner*, Eric Gloaguen and Michel Mons*

LIDYL, CEA,CNRS, Université Paris-Saclay, bât 522, CEA Paris –Saclay, 9119 Gif-sur-Yvette, France

Abstract

Natural Bond Orbital (NBO) analysis of electron delocalization in a series of capped isolated peptides is used to diagnose amide-amide H-bonding and backbone-induced hyperconjugative interactions, and to rationalize their spectral effects. The sum of the stabilization energies corresponding to the interactions between NBOs that are involved in the H-bonding is demonstrated as an insightful indicator for the H-bond strength. It is then used to decouple the effects of the H-bond distance to that, intrinsic, of the donor/acceptor relative orientation, i.e., the geometrical approach. The diversity of the approaches brought by the series of peptides studied enables us to illustrate the crucial importance of the approach when the acceptor is a carbonyl group, and emphasizes that efficient approaches can be achieved despite not matching the usual picture of a proton donor directly facing a lone pair of the proton acceptor, i.e., that encountered in intermolecular H-bonds. The study also illustrates the role of backbone flexibility, partly controlled by backbone-amide hyperconjugative interactions, in influencing the equilibrium structures, in particular by frustrating or enhancing the HB for a given geometrical approach. Finally, the presently used NBO-based HB strength indicator enables a fair prediction of the frequency of the proton donor amide NH stretching mode, but this simple picture is blurred by ubiquitous hyperconjugative effects between the backbone and amide groups, whose magnitude can be comparable to that the weakest H-bonds.

1. Introduction

The amide-amide H-bonding is a key interaction of proteins and bioinspired polymers, like foldamers, often considered at the heart of the stability of their secondary structures.[1-4] During the folding process, proteins NH donor sites seek to satisfy their propensity to form H-bonds (HBs) by finding an acceptor partner CO site leading to intramolecular H-bonding: this feature is even invoked as the main driving force to protein folding.[5, 6] Thus early H-bonds biochemists have recognized that the most iconic secondary structures of proteins, such as the α-[3, 4] or 3_{10} helices[4], β-turns [7] or 2_7 ribbons[4, 8] are stabilized by H-bonds, namely the so-called C13, C10 or C7 H-bonds (labelled according to the length of the ring formed). Even extended peptide conformations like β-strands can be considered as stabilized by such a C5 interaction, as recently surmised from a protein survey.[9] Knowledge of these H-bonds has greatly benefited from the characterization of isolated model systems, mostly capped aminoacids or peptide building blocks, composed of complete peptide links, which interact with each other, without perturbations other than those induced by the backbone residues of the sequence.[10, 11] In particular such an approach enables to focus on the intrinsic H-bonding, without involvement of neighbouring H-bonds (absence of cooperative effects) or of the environment (no solvent effect).

Thus in recent gas phase experiments[12] spectroscopists have recorded conformation-selective spectra in the IR and the UV range, making possible the determination of the most stable conformations in flexible molecules, like peptides or foldamer building blocks, and the characterization of their H-bonding content. The wealth of data collected using laser spectroscopy during the past decade[10, 11, 13-19] constitutes an extended set of peptide conformations, with both natural[14, 20-29] and synthetic β-[17, 18, 30] or γ-[31, 32]peptides, in which two amide groups interact with each other, according to a panel of geometrical approaches modulated by covalent constrains imposed by the peptide backbone. This conformational set can be considered as a sampling of possible amide-amide geometrical approaches, mimicking those encountered in the desolvated inner core of proteins.[33] These experimental studies stem from a synergetic action with theoretical approaches, which have greatly improved since the early days of peptide quantum modelling[34, 35] and can nowadays efficiently handle dispersive interactions, which are ubiquitous in these systems.[36-38] The IR spectra are assigned by comparison with quantum chemistry calculations of vibrational modes and conversely the good agreement usually achieved enables an assessment of the quantum chemistry methods chosen.[39] The observable of choice in these gas phase optical experiments is the spectral transition of the NH stretch vibration, since the usual HBs are characterized by unique features,[40] namely, i) a red-shifted frequency of the NH stretch reflecting the weakening of the NH covalent bond, ii) an enhancement of the band intensity of this mode due to the polarization of the NH proton donor moiety and iii) a partial electron delocalization (charge transfer) from the HB acceptor to the NH moiety.

A striking observation within the library of H-bonded amides evoked above is that the spectral shifts recorded are sometimes much larger than that measured on a natural reference for two interacting amide groups, namely the dimer of the methylacetamide (MAA) molecule, whose spectroscopy has been recently revisited.[41, 42] In this latter system, indeed, the limited contact between the two amides groups allow them to interact in the most efficient way to form a strong, natural HB, which results

from an electrostatic-polarization component, also potentially influenced by a dispersive component[37, 39] and some partial charge transfer (CT) as well.[43, 44] Conversely, when the amides belong to the same molecule, the set of geometrical approaches available is limited, leading to a significant frustration of the H-bonding. In this respect, the observation of larger red shifts in some intramolecular cases, compared to the intermolecular one, may appear paradoxical since they would correspond to an enhancement of the H-bond with respect to the reference dimer. Moreover, such large red shifts can also correspond to the vibrational signature of free NH bonds, undergoing hyperconjugation (HC) from vicinal or neighbor orbitals[45, 46] (Bohlmann effect[47]) as it has been recently illustrated on isolated model hydrazides.[48]

The aim of the present benchmark study is to rationalize the diversity of H-bonding strengths observed within a set of peptide secondary structures, to understand why several peptides exhibit unusually red shifted H-bonds and eventually assess the role of the peptide environment (comprising both backbone and main chain) in determining the HB strengths. Beyond the use of vibrational red shifts by spectroscopists, a rigorous analysis of the local electron densities can provide a convenient and effective framework for both diagnosing the presence of H-bond and gauging their strength. The methodology chosen, however, has to meet some essential requirements. First, it must enable a clear diagnostics of the H-bond while being readily applicable to different approaches with a broad spectrum of nearby environments. Second, it must enable the electronic wavefunction to be expressed in a localized language, without making any assumptions about its mathematical form, and should transcript accurate calculations into chemical insights about H-bonding. Finally, the method must distinguish the intrinsic HB features from hyperconjugative effects not directly linked to the HB itself. In this respect, one will notice that, despite HB itself is sometimes viewed or interpreted as an hyperconjugative effect,[45, 46] in the present paper the term HC will exclude HB contributions. These criteria lead to choose the natural bond orbital (NBO) method,[49-51] in which the electronic wave function is analyzed in the framework of localized Lewis-like chemical bonds. Based on local block eigenvectors of the one-particle density matrix, and developed to study hybridization and covalency in polyatomic wave functions, this method and its principles have been extended to treat the so-called “van der Waals bonding”, in particular inter- and intra-molecular HBs (see for example: Refs. [52-57]). The strategy implemented in this work stems from the NBO analysis[49-51] of the electronic structure of a set of peptide secondary structures, starting from unconstrained amide-amide HBs, as revealed by MAA dimers (a system also previously investigated by Adhikari & Scheiner[37] using a NBO analysis), and then comparing them with those encountered in typical peptide building blocks and secondary structures, namely models of the γ- turn and β-strand structures. It will be shown that a general specific feature of the NBO stabilization energies related to the HB formation, namely its dependence with the HB distance, can be used to rank the strengths of the amide-amide HBs observed in peptides and to assess the role of the peptide environment on the structure. Finally, the issue as to whether the NH stretch frequency is a good marker of the HB strength is also addressed, through its correlation with the HB strength, as obtained from NBO analysis, together with the role of hyperconjugative interactions[45, 46] between the NH bond considered and vicinal/neighbour orbitals.[45, 46, 48]

2. Methodology

2.1 Benchmark set composition

The present benchmark study is focused on specific conformations of a series of model diamide molecules completed by a few tri- and tetra-amides, all featuring as much as possible isolated HBs, for which the amide bonds involved in the HB considered are either single proton donor or single proton acceptor moieties. It encompasses data on *trans*-methylacetamide (MAA) dimers,[41, 42] basic amino acids (AA), Ala, Gly, Phe, Aib (amino isobutyric acid),[14, 20, 23, 27, 29] some di- and tri-peptides of these AAs,[21, 22, 24, 25] as well as synthetic AAs (β- and γ-aminoacids).[17, 30, 31] All these peptides are capped to form complete amide units, apart from one hydrazide group in an aza-compound.[30] The model caps considered are those present in the gas phase experiments as well as more simple counterparts (acetyl and methylamide caps) in order to assess their influence on the peptide structure.

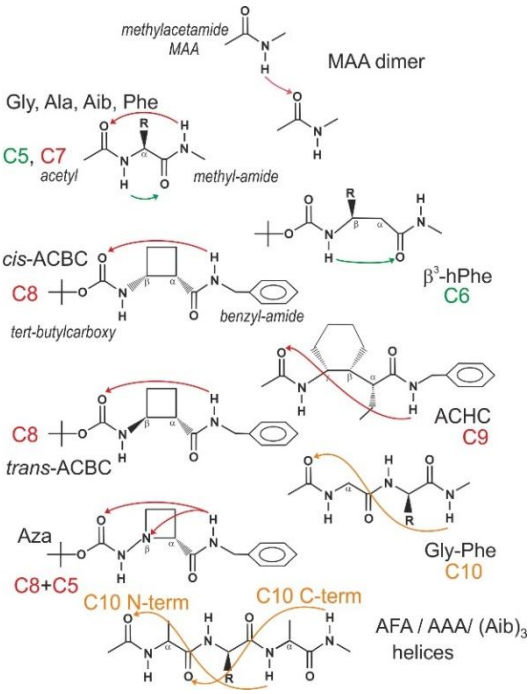


Figure 1: Set of specific conformations of model molecules considered in the present work, closely related to experimental data on t-MAA dimers, capped α-, β- and γ-peptides (see text). The stabilizing HBs are indicated by arrows, together with the terminology used (number of atoms in the ring closed by the HB and short names of the molecules).

Most of the conformations considered (Fig. 1) were observed in microwave[58, 59] or in conformer-selective laser spectroscopic gas phase experiments.[14, 17, 20-25, 27, 29-31] The theoretical structures, calculated in the present study, have been determined using a DFT-D method, at the B97D3(BJ)-abc/def2-TZVPPD level of theory,[60-62] together with harmonic vibrational frequencies, using the TurboMole package.[63] Fig. 2 illustrates the fair correlation obtained this way between experimental NH stretch frequency data and their theoretical counterparts, showing that a good description of the NH stretching mode is achieved at this level of theory.

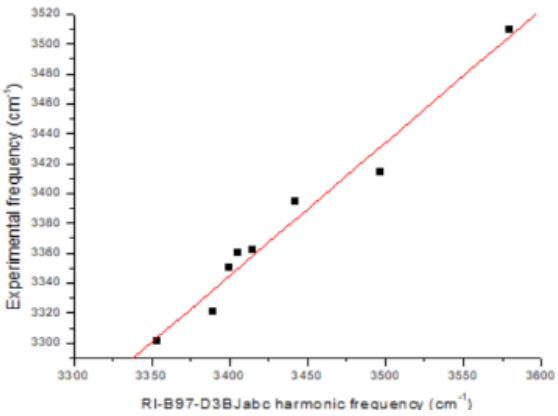


Figure 2: Correlation between experimental NH stretch frequencies as measured in IR/UV conformer-selective gas phase experiments and harmonic frequencies at the B97D3(BJ)-abc/def2-TZVPPD level of theory.

2.2 NBO analyses and diagnostics:

After a brief reminder of the main valency and bonding concepts of the NBO method,[45, 46, 49-51] its application to diagnose the presence of a HB will be illustrated on the inverse γ-turn form of the Ala diamide.[59] However, before this, intrinsic amide-backbone hyperconjugative effects, already present in the absence of HB, will be assessed on a relevant conformation of the related model molecule possessing a unique amide group, namely the *N*-isopropylacetamide.

2.2.1 Nomenclature and computational details:

The NBO-based chemical bonding concepts rest on an expression of the molecular properties in terms of a 'natural Lewis structure' depiction of the wavefunction. The wavefunction is optimally transformed into a localized form corresponding to the one-centre ("core" or "lone pair") and two-center "bond" elements of the chemist's Lewis structure picture. The various natural localized sets can be considered as resulting from a sequence of transformations of the input orbital basis set. The NBOs are obtained as local block eigenfunctions of the one-electron density matrix and have optimal convergence properties for describing electron density. They are partitioned into high- and low-occupancy orbital types: the small set of most highly-occupied orbitals contains the core and valence (bond-antibond) functions and are distinguished from the weakly occupied "Rydberg" (extra-valence-shell) functions. The symbols "x" and "x*" will be used to refer to filled and unfilled orbitals of the formal Lewis structure, x being either core orbitals (c), lone pairs (n), σ or π bonds (σ, π), and x* being either σ or π antibonds (σ*, π*) or extra-valence Rydberg (Ry) orbitals. The calculation of the donor-acceptor interactions in the NBO basis is carried out by examining all possible interactions between "filled" (donor) Lewis-type NBOs and "unfilled" (acceptor) non-Lewis NBOs and estimating their energetic importance by 2nd order perturbation theory. The filled NBOs of the "natural Lewis structure" are well adapted to describe covalency effects whereas the unfilled in the formal Lewis and in particular, the antibond NBOs, are well adapted to describe non covalency effects. For each donor NBO (i) and acceptor NBO (j), the stabilization energy E(2) associated with delocalization is calculated as:

$$\mathrm{E}(2) = \Delta E_{ij} = q_i \frac{F(i,j)^2}{\epsilon_i - \epsilon_j}$$

where q_i is the donor orbital occupancy, ϵ_i, ϵ_j are diagonal elements (orbital energies) and $F(i,j)$ is the off-diagonal NBO Fock matrix element.

The NBO analysis[50] has been carried out on the B97D3(BJ)-abc/def2-TZVPPD equilibrium structures at both the HF/TZVPP and MP2/TZVPP levels using the NBO module[64] in the Gaussian 16 package.[65] The HF/TZVPP level is only used to generate the first step of the calculation of the stabilization energies; the natural population analysis (NPA) charges and the NBOs occupancies considered in the following being that obtained at the MP2/TZVPP level. It has been demonstrated on a set of small systems that this level of theory is sufficient and gives results similar to those obtained at more sophisticated levels such as MPSDQ or QCISD.[48] For the E(2) stabilization energies, the thresholds for considering the interactions as significant were 0.05 kcal/mol for the intermolecular interactions and 0.5 kcal/mol

for the intramolecular ones, except in some specific cases (weak interactions), where it was necessary to reduce it down to 0.1 kcal/mol.

2.2.2 H-bond and hyperconjugation diagnostics: the inverse γ-turn form of the Ala diamide and the related N-isopropylacetamide conformation.

Before performing the NBO analysis on the inverse γ-turn form of the Ala diamide, the *N*-isopropylacetamide (N-propan-2-ylacetamide), a model molecule in which the C-terminal side of the Ala diamide is substituted by a methyl group, was first investigated in order to reveal the contribution of hyperconjugation effects, already present in absence of any H-bonding, and thus to allow in the following a clear discrimination between these HC effects and HB formation (Figure 3).

The equilibrium structure of the *N*-isopropylacetamide conformation, that is directly comparable to the Ala diamide γ-turn conformation (Figure 3 a and b), exhibits a *N*-terminal geometry with a $C^{\alpha}H$ ---O(1)C distance of 247 pm, typical of a close contact and comparable to the average contact distance found in crystals : 248 pm (according to the survey by Rowland and Taylor[66]), together with a φ Ramachandran dihedral of -86°. NBO analysis (Table S1, in supplementary information) provides evidence for significative hyperconjugative interactions enabling us to rationalize these structural features. The strongest HC interaction (E(2) = 9.0 kcal/mol) involving amide groups and backbone covalent bonds corresponds to an electron delocalization resulting from the overlap of the NBO lone pair (donor) localized on the nitrogen atom, identified as $n_{N(1)}$, with the NBO antibond (acceptor) localized on the vicinal CαC(2) bond, identified as $\sigma^*_{C\alpha C(2)}$, referred to as a $n_{N(1)} \rightarrow \sigma^*_{C\alpha C(2)}$ interaction (see Figure 3c). This interaction enables the amide group to strongly affect the orientations of the covalent bonds involving the Cα atom: an optimum overlap of these two NBOs favors a φ = -90° geometry and locks the structure of the backbone N-terminal side, in line with the Ramachandran dihedral of φ = -86° calculated. Two smaller interactions involving the same nitrogen and the Cα atoms are also detected (HC0 set in Table S1): a $n_{N(1)} \rightarrow \sigma^*_{C\alpha H}$ interaction of 2.4 kcal/mol and a $n_{N(1)} \rightarrow \sigma^*_{C\alpha C\beta}$ interaction of 2.2 kcal/mol, due to a lesser NBO overlap.

As far as delocalisation to the $\sigma^*_{N(1)H}$ NBO is concerned, two significant hyperconjugative interactions are detected, a $\sigma_{CO(1)} \rightarrow \sigma^*_{N(1)H}$ interaction of 1.8 kcal/mol and a $\sigma_{C\alpha H} \rightarrow \sigma^*_{N(1)H}$ interaction of 4.4 kcal/mol (HC1 set in Table S1). The first one is internal to the peptide bond and contributes to the planar structure of the motif, whereas the latter, more importantly describes the tendency of the vicinal NH and CαH bonds to adopt an antiparallel orientation (Figure 3d). These interactions result in a modest but significant NBO population of the $\sigma^*_{N(1)H}$ NBO, namely ~34 10^{-3} *e* (10^{-3} *e* will be referred to as m*e*, milli-*e*, in the following). One can also notice that no interaction (with E(2) > 0.1 kcal/mol) corresponding to an eventual $C^{\alpha}H$---O(1)C HB such as a $n_{O(1)} \rightarrow \sigma^*_{C\alpha H}$ interaction could be detected.

The NBO analysis of the inverse γ-turn form of the Ala diamide (Figure 3 b) demonstrates that delocalization within the N(2)H---O(1)C amide-amide HB results from an overlap between three donor NBOs, located on the CO(1) carbonyl, and the acceptor antibond $\sigma^*_{N(2)H}$ NBO, localized on the

N(2)H group. (Table S1, bottom) (one will notice that donor NBOs are located on the HB proton accepting moiety whereas the acceptor orbital pertains to the HB donor NH). Two of the donor NBOs correspond to lone pairs of the O(1) oxygen atom (n_O and n'_O), which exhibit different mixed *sp* characters: the n_O NBO is of mixed character, 62% of *s* character for 38% of *p* character (Fig. 3g), whereas n'_O is of pure *p* character (99%; Fig. 3f). The third donor orbital involved in the HB is the $\pi_{CO(1)}$ NBO, localized on the

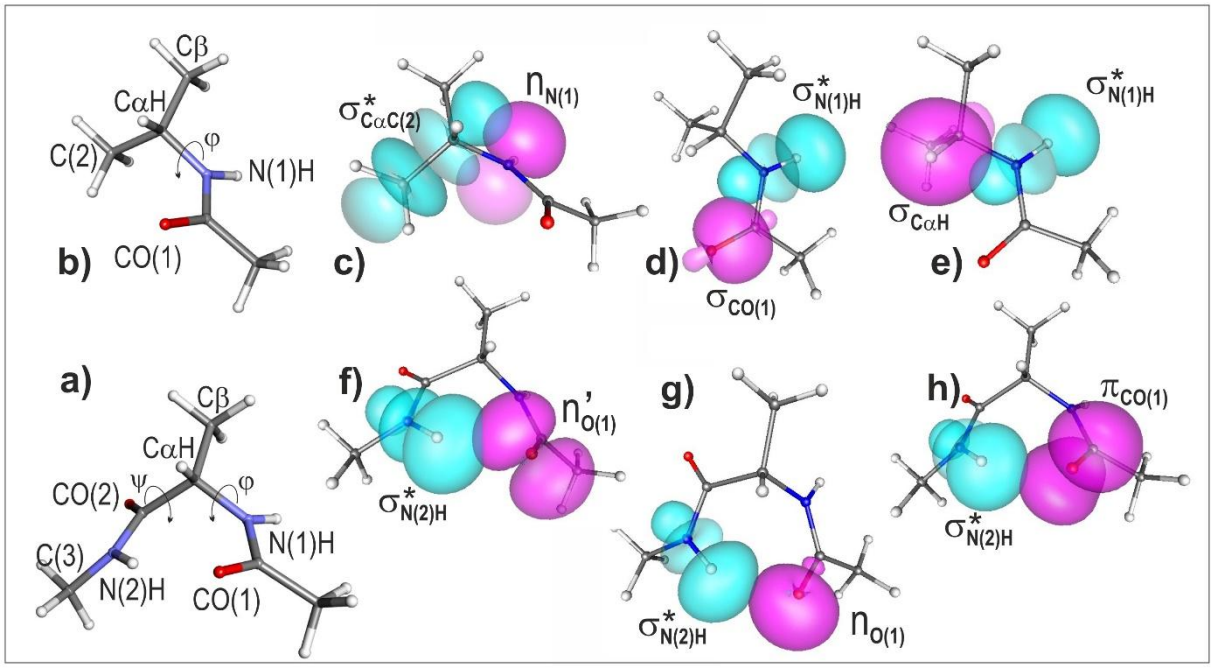


***Figure 3: Left part*: Quantum chemistry structure (at the B97D3(BJ)-abc /def2-TZVPPD level of theory) of *a)* the inverse γ-turn conformation of the Ala residue, with acetyl and methyl amide caps, and of *b)* the corresponding conformation in the *N*-isopropylacetamide molecule, in which the C-terminal side of the Ala diamide is substituted by a methyl group. Relevant atomic and dihedral notations are also displayed. *Right part* : Natural Bond Orbitals, generated from NBO analysis of the two molecules, illustrating the overlaps between electron density donor (magenta) and acceptor (cyan) orbitals corresponding to a series of interactions : in N-isopropylacetamide (top): *c)* $n_{N(1)} \rightarrow \sigma^*_{C\alpha C(2)}$ interaction responsible for the φ ~ 90° Ramachandran dihedral, *d)* $\sigma_{CO(1)} \rightarrow \sigma^*_{N(1)H}$ and *e)* $\sigma_{C\alpha H} \rightarrow \sigma^*_{N(1)H}$ interactions (magenta), these two latter contributing to a basic population of the $\sigma^*_{N(1)H}$ NBO. In the Ala inverse γ-turn model, *f-h)* the $n_{O(1)} \rightarrow \sigma^*_{N(2)H}$, $n'_{O(1)} \rightarrow \sigma^*_{N(2)H}$ and $\pi_{CO(1)} \rightarrow \sigma^*_{N(2)H}$ interactions, which correspond respectively to the three CO(1)-based donor (magenta) NBOs, donating to the σ* NBO (cyan) located on the N(2)H covalent bond of the HB donor amide.**

CO(1) carbonyl group (Fig. 3g). The overlap of each of these donor NBOs with the acceptor $\sigma^*_{N(2)H}$ gives rise to significant E(2) stabilization energies of 1.3, 2.5 and 1.0 kcal/mol for the $n_{O(1)}$, $n'_{O(1)}$ and $\pi_{CO(1)}$ NBOs, respectively. In order to account for all these components, the sum ($\sum E_{HB}$) of the individual E(2) stabilization energies, associated to the $n_{O(1)}$, $n'_{O(1)}$ and $\pi_{CO(1)}/\sigma^*_{NH(2)}$ overlaps involved

in the N(2)H---O(1)C HB and obtained from the NBO analysis (4.8 kcal/mol), has been taken as a HB strength indicator.

Additionally, the same analysis also enables us to characterize the strongest hyperconjugative interactions that take place between backbone and/or side chain (SC) NBOs. In the diamide system, we indeed observe hyperconjugative interactions of the same nature than those found in the *N*-isopropylacetamide model molecule (see Table S1):

(i) three interactions between each of the $n_{N(1)}$ and $n_{N(2)}$ NBO donors and three specific NBO acceptors. The $n_{N(1)}$ NBO interacts with Cα atom-based NBOs, the $\sigma^*_{C\alpha C(2)}$, $\sigma^*_{C\alpha H}$ and $\sigma^*_{C\alpha C\beta}$ NBOs, resulting in a sum of individual E(2) energies, $\sum$E(2), of 14.4 kcal/mol (the first one being still prominent at 10.1 kcal/mol; Table S1, HC0 set). Similarly the $n_{N(2)}$ NBO donor interacts with NBO's involving the C-terminal cap carbon atom (C(3)), the three $\sigma^*_{C(3)H}$ NBOs, resulting in a similar $\sum$E(2) of 15.4 kcal/mol. These interactions contribute to control of the orientations of the covalent bonds established by the C atoms directly after each amide group along the peptide chain, namely the Cα atom and the C(3) atom of the C-terminal cap., and

(ii) two interactions involving each of the $\sigma^*_{N(1)H}$ and $\sigma^*_{N(2)H}$ NBO acceptors, namely the $\sigma_{CO(1)} \rightarrow \sigma^*_{N(1)H}$ and $\sigma_{C\alpha H} \rightarrow \sigma^*_{N(1)H}$ interactions of 1.7 and 3.5 kcal/mol resp. (Table S1, HC1 set) and the $\sigma_{CO(2)} \rightarrow \sigma^*_{N(2)H}$ and $\sigma_{CH(3)} \rightarrow \sigma^*_{N(2)H}$ interactions of 1.7 and 3.7 kcal/mol resp. . The $\sigma_{CO} \rightarrow \sigma^*_{NH}$ interactions are internal to the peptide bonds, whereas the $\sigma_{CH} \rightarrow \sigma^*_{NH}$ incline the vicinal NH and CH bonds to adopt an antiparallel orientation.

The HB interactions and the latter hyperconjugative interactions lead together to a $\sigma^*_{N(1)H}$ NBO population of ~33 m*e*, similar to that obtained for the *N*-isopropylacetamide molecule, but to an increased population of the $\sigma^*_{N(2)H}$ NBO, ~43 m*e*, providing clear evidence for the N(2)H---O(1)C HB formation.

Such an analysis and discussion has first been tested on the simplest intermolecular HB system, i.e., the methylacetamide dimer, and then extended to intramolecular HB systems, within a series of model diamide or triamide molecules; the purpose being to discriminate the different HBs from hyperconjugation effects. In addition, the sum $\sum E_{HB}$ as well as the population of the σ^*_{NH} involving in the HB have been used for documenting the behavior of the NH stretch frequency.

3. Intermolecular amide-amide interactions as modelled by MAA dimers

The NBO analysis presented above has been applied to the most natural system in which two non-covalently bound amide groups interact through a HB, namely the *trans*-methylacetamide dimer. Starting first from the equilibrium structures obtained by quantum chemistry, the analysis procedure has then been extended to a series of elongated or compressed HBs, sharing the same geometrical approach, i.e., the relative orientation of the donor and the acceptor amides.

3.1. MAA dimers

The conformational landscape of the H-bonded dimer of the *trans*-methylacetamide model molecule (MAA), recently investigated at a high level of theory (MP2/aug-cc-pVDZ ; geometry optimization

with counterpoise corrections) by Adhikari and Scheiner[37], exhibits several minima, namely two types of H-bonded conformations and one stacked form of lesser stability. The present theoretical investigation (B97D with D3(BJ)-abc corrections), focused on the H-bonded dimers, is in qualitative agreement with these findings. The HB distances, for instance, are found to be closer to those obtained by Adhakari and Scheiner with a counterpoise-corrected optimization than without (see Table S1 and Supp. Info of

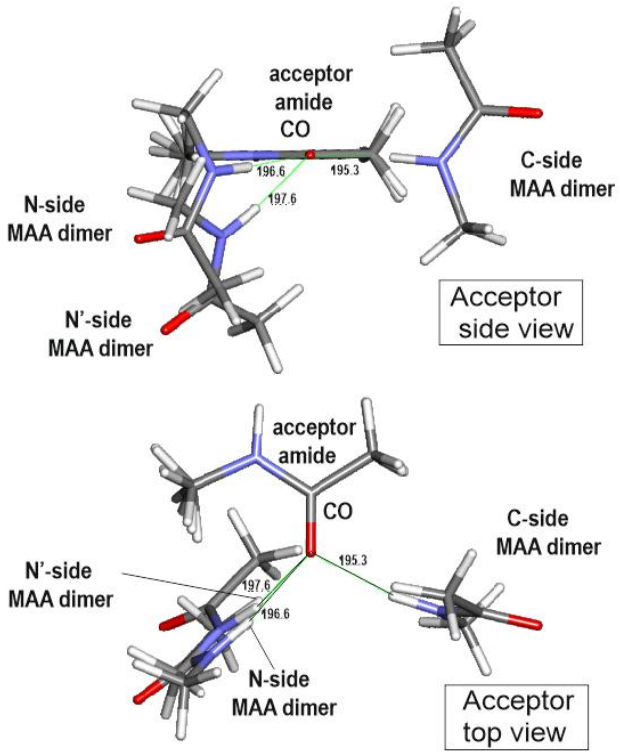


Figure 4: Sketch of the two types of MAA H-bonded dimers, in which the HB acceptor molecules are overlaid : top and bottom panels correspond to acceptor side and top views respectively. The donor molecule is located either on the C-side or on the N-side of the acceptor molecule and has its NH close to the acceptor plane (referred to as C- and N-side dimers), or is on the N-side but tilted relative to the acceptor (N'-side dimer). Interatomic HB distances (B97D3(BJ)-abc/def2-TZVPPD level of theory) are given in pm.

Ref. 37), in agreement with the negligible BSSE expected with the DFT framework associated to this level of basis set (def2-TZVPPD) and justifying geometry optimizations carried out without BSSE-correction in the present work. Two types of H-bonded dimers (Fig. 4) are found: they both exhibit a linear H-bond, with the NH bond of the donor molecule pointing towards the acceptor carbonyl O atom, but they differ by the side of the H-bonding approach. One type has its MAA-donor molecule in close contact with the acetyl moiety of the MAA-acceptor and is referred to as the C-side dimer (right hand-side in Fig. 4.). The donor NH exhibits a side position (CO-H angle $\theta_{CO\text{-}H}$ = 118° in the present data, 120° in ref 37, See Fig. S1 for the definition of the angles and dihedrals), very close to the plane of the proton acceptor amide ($\varphi_{H\text{-}OCN}$ ~180°, θ' ~0°). In contrast, the other type of dimer has its donor in contact with the NHMe moiety (left hand-side figure 4). A first N-side conformer exhibits a linear HB, with its donor NH located close to the acceptor amide plane ($\varphi_{H\cdot OCN}$ = -6°, and -11° in Ref 37 and in the present work respectively) but less tilted from the carbonyl axis compared to the C-dimer, (CO-H angle $\theta_{CO\text{-}H}$ = 138° and 142° in the present work and in 37 respectively). The method presently used, however, also leads to a second N-side stable conformer, referred to as N'-side, and characterized by a linear HB (Fig. 4). Its NH donor is significantly shifted above the amide plane ($\varphi_{H\text{-}OCN}$ = +44°), but the angle of approach to the acceptor ($\theta_{CO\text{-}H}$ = 126°) is comparable to that of the C-dimer ($\theta_{CO\text{-}H}$ = 118°). In this N'-side conformer, the relative orientation of the two amides is also

significantly tilted ($\varphi_{CN\text{-}OC}$ = -40°) compared to the two latter forms, which have their amide planes nearly perpendicular ($\varphi_{CN\text{-}OC}$ = -75° and -71°, see Supp. Info). As far as relative stability is concerned, the two N- and N'-side dimer conformations are found to be nearly isoenergetic (within 0.2 kcal/mol, see Table S2), illustrating the relative flatness of the potential energy surface in the N-side region. One should notice that for the present investigation, focused on the dependence of the H-bonding upon the relative orientation of the donor and acceptor moieties (see Section 3), the issue of the real existence of a minimum at the N'-side geometry, which was not reported by Adhikari and Scheiner, is not critical, since the NBO analysis can be carried out whatever the geometrical conformation, be a minimum or not. Additionally, this N'-side dimer is also interesting for the presently studied issue, since it suggests to consider an alternative orientation of the two amides, differing from that of the C- and N-side dimers.

Concerning the comparison with protein data, the approaches of the donor to the acceptor amide, observed in the dimers, characterized by φ' angles ranging between 120° (C and N') and 140°(N) and θ' between ~0° (C and N) and 35° (N'), are comparable to those obtained from a protein survey[33] whose (symmetrized) distributions peak at φ' ~125° and θ' = 0° respectively (See Supp. Info for φ' and θ' angle definition).

From a structural point-of-view, the present results suggest that there exists three possible quasi-isoenergetic HB approaches of an amide to another amide, one with the donor on the C-side of the acceptor, and two on the N-side, characterized by similar HB equilibrium distances (Table S2). The NBO analysis of the three dimers has been carried out in order to characterize the delocalization associated to HB formation. C- and N-side dimers exhibit NBO overlaps between NBO lone pairs of the oxygen atom (n_O and n'_O) of the CO group of the HB acceptor amide, and the antibond NBO σ^*_{NH} localized on the NH group of the HB donor amide. Each of these interactions gives rise to significant E(2) stabilization energies in the C- (Table S3) and N-dimers: 3.3 and 4.3 kcal/mol resp. for the $n_O \rightarrow \sigma^*_{NH}$ interaction, and 6.6 and 3.8 kcal/mol resp. for the $n'_O \rightarrow \sigma^*_{NH}$ interaction. In contrast the N'-side dimer, with its NH donor located off the amide plane, benefits from three overlaps, those corresponding to the $n_O/n'_O \rightarrow \sigma^*_{NH}$, with E(2) = 3.6 and 2.7 kcal/mol resp., and a third one, of $\pi_{CO} \rightarrow \sigma^*_{NH}$ type, with E(2) = 1.1 kcal/mol (Table S4). The sum of the stabilization energies associated to HB formation ΣE_{HB} in the three C, N and N' dimers give rise to decreasing values of: 9.9, 8.4 and 7.4 kcal/mol resp., suggesting decreasing HB strengths. These values are in qualitative agreement with those derived by Adhikari and Scheiner for the MP2 structures of C and N dimers (See Table S2) and are stronger than the value obtained for the inverse γ-turn of Ala (4.8 kcal/mol ; Section 2.2.2). The ΣE_{HB} values obtained also agree well with the populations of the σ^*_{NH} NBOs, which amount to 48, 45 and 45 m*e*, for the C-, N- and N'-dimers respectively. As expected they are much larger than the reference value for the free amide, i.e. ~34 m*e* in the Ala γ-turn (see Section 2.2.2) and 31-32 m*e* for the HB acceptor *trans*-methylacetamide molecule in the C and N' dimers (Tables S3 and S4). They are even larger than that of the inverse γ-turn of Ala (43 m*e*). Eventually, the NBO analysis also provides the net charges of both donor and acceptor moieties, which reveal an effective electron transfer of 23 and 19 m*e* at the equilibrium geometry of the C and N' dimers (Tables S3 and S4), in qualitative agreement with the values of the two indicators, the sum ΣE_{HB} and the σ^*_{NH} NBO population.

Coming back to the energetics, one can notice that despite a significant difference in H-bonding strengths, the three dimers exhibit very similar H-bonding distances as well as similar energetics (within less than 0.2 kcal/mol, Table S2). They correspond to different approaches of a donor amide to an acceptor, on either side of the carbonyl acceptor, in or out of the amide plane. Obviously, the several interactions, other than the H-bonds, present in these three species differ substantially. In particular, whereas the C-side dimer donor does not experience any close contact with the acceptor C-side, the situation is different for the N-and N'-side dimers. In the N-side species, an NH in-plane approach of the acceptor with a $\theta_{CO\cdots H}$ angle comparable to that of the C-dimer (120°) would be hampered by a steric clash between the donor N-atom and the N-terminal methyl of the acceptor, eventually resulting in a larger θ_{CO-H} (140°). This forbids an approach that would mirror, on the N-side, that of the C-side dimer, and as a result, the N-side dimer features a lesser delocalization and then a weaker H-bonding. Interestingly, the N'-side dimer can be seen as a trick of the system to overcome this difficulty: tilting the donor NH out of the amide plane in N' enables the recovery of a small θ_{CO-H} angle, while keeping the NBO overlap significant. The similar energetics of the three forms, however, suggests that other attractive interactions in N and N' compensate for the decrease in HB strength, namely electrostatics, induction and dispersion; the latter being favored by close contacts.

Finally, NH stretch frequency calculations indicate that the C-side dimer exhibit the larger red-shift (by ~ 31 and 36 cm^{-1} compared to N' and N-side dimers respectively, see Table S2), suggesting a slightly stronger H-bond than its N- and N'-side counterparts. Likewise, the C-side dimer tends to exhibit a shorter H-bond distance than its N- and N'-side counterparts, by 0.6 or 1.3 pm, depending on the method considered (MP2 in Ref 37 or DFT-D in the present results; Table S2). These theoretical data agree well with the NH-stretch spectroscopic data of MAA in a supersonic expansion, which have been reinterpreted in terms of simultaneous presence of two H-bonded dimers of *trans*-MAA molecules, whose mid-IR spectral signatures (red-shifted NH bands) differ by 31 cm^{-1}.[42]

3.2. Ranking the efficiencies of amide-amide approaches: decoupling the H-bonding strength from the intermolecular distance

The observation of MAA dimers with different geometrical approaches raises the question of the intrinsic strength of these H-bonding approaches and of their relative ranking. Broadly speaking, one can anticipate that the strength of any H-bond depends on both i) the relative orientation of the two amide groups, i.e. the geometrical approach made possible/allowed by the backbone constrains, and ii) the H-bonding distance. Thus ranking the intrinsic efficiencies of the HB approaches requires the decoupling of the HB strength from the distance parameter. For this purpose the dependence of the HB strength upon the intermolecular distance has been obtained for the C- and N'-side MAA dimers, whose geometrical approaches differ radically. A NBO analysis has been carried out to determine the ΣE_{HB} indicator on a series of geometrical structures belonging to the same approach, i.e. for a series of fixed HB distances around the equilibrium structures, with a frozen relative orientation of the amide groups (acceptor CO-donor-NC_{amide} dihedral), the other degrees of freedom being optimized.

Figure 5 shows that for a given geometry approach, that of the C- or N'-side dimer, the sum of the stabilization energies corresponding to H-bonding (ΣE_{HB}) are nearly aligned along a straight line in a

semi-log plot (red and magenta dots) when the HB distance is varied, suggesting an exponential-type behavior in the range of distances considered. Although remarkable, this result is not so easy to rationalize. Each of the two-orbital E(2) interactions obtained from the NBO analysis depends on the overlap between the NBOs involved in the interaction together with the NBO energy difference (expression of E(2) in Section 2.2.1), both depending on the distance in a specific way. The apparent

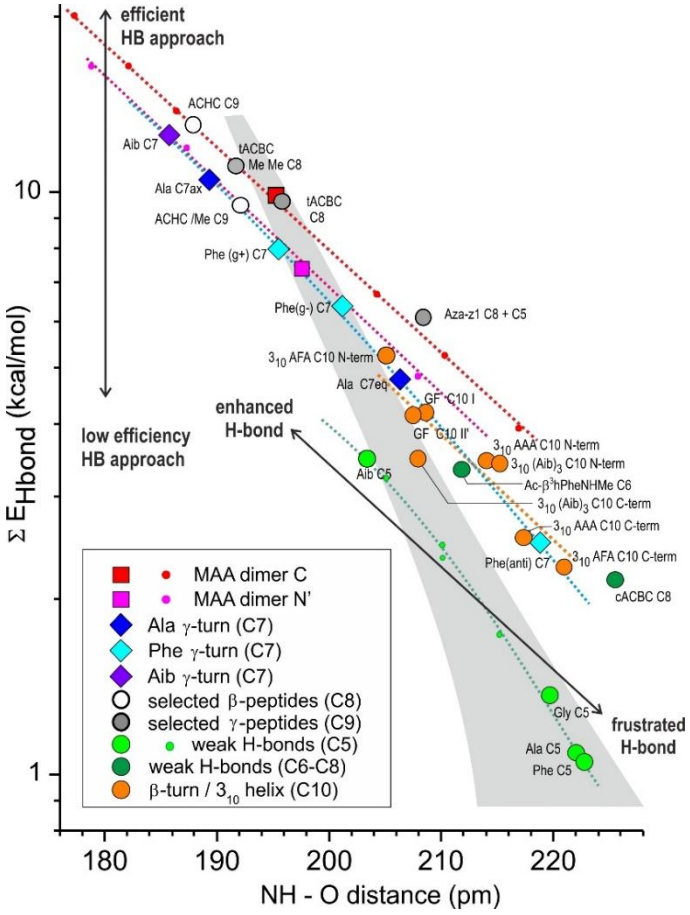


Figure 5: Semi-log plot of the sum of the HB stabilization energies ($\sum E_{HB}$), as obtained from the NBO analysis of the amide-amide HB, in the C- and N'-side dimers of *trans*-methylacetamide and in a series of conformations of di, tri- or tetra-amide molecules, as a function of the H-O distance (see also Tables S3, S4 and S5). Large symbols stand for equilibrium structures whereas small symbols correspond to squeezed or elongated dimers or C5 structures (see Section 4.2). A full identification of the NH-OC interactions is provided in Table S5 of the Supp. Info., from the abbreviated identifiers. The dotted lines feature a given H-bonding approach, along which struct[redacted]roach are expected to be aligned (see Sections 3.2, 4.1, 4.2 and 5.1): the lower the line, the less efficient the geometrical approach. Within a given approach (dotted lines), equilibrium structures found on the right-hand side correspond to frustrated HBs, and those on the left-hand side to enhanced HBs. The grey area is associated to a neutral region, where the peptide environment is not expected to significantly affect the HB strength (See Discussion in Section 5.2).

quasi-exponential dependence of the sum of those stabilization energies involved in the H-bonding (ΣE_{HB}) presumably results from a subtle sum of specific behaviors involving different pairwise two-orbital interactions in the particular range of distances considered.

Fig. 5 also shows that both dimers obey parallel dependences in the semi-log plot: the N'-side MAA dimer (magenta dots) lying below that of the C-side dimer (red dots), showing that the former approach is intrinsically less efficient than the latter to establish a HB. As already mentioned above, this apparent penalty can be assigned to the steric hindrance between both amides (in particular the methyl amide side of the HB acceptor and the π cloud of the HB donor), which restricts the set of accessible conformations and can forbid geometries most favorable to HB formation. One can notice that, despite a significant difference in HB strength, the dimers remain isoenergetic (Table S2), which justifies focusing our analysis on a local approach, such as the ΣE_{HB} indicator deduced from the NBO analysis, in order to distinguish the HB strengths.

The present semi-log plot E_{HB} vs. H-bonding distance of Fig. 5 appears then as an efficient and fast tool to rank the efficiency of any HB approach relative to the dimers. This can be done by considering the vertical distance of its point to the dimer considered, in the diagram of Fig. 5, whatever the structure chosen to evaluate the H-bond strength of this approach, being an equilibrium geometry or not. In other words, this plot decouples the intrinsic strength of the approach (i.e., its H-bonding efficiency, which is linked to the capability to give rise to electron delocalization and therefore depends upon the approach geometry) from its dependence with the H-bonding distance.

The aim of the present work is to extend the methodological procedure, introduced on the non-covalent dimers, to covalently linked amides, e.g. peptides, expecting that consistent series of conformations having similar geometries (case of the Ala, Phe and Aib γ-turns,[36] see Figure 1 and next Section) are representatives of the same approach and thus exhibit the same HB efficiency. The goal of the following sections will be to collect the HB strengths along such consistent series and to compare them to the dimer behavior in the semi-log plot of Fig. 5. The position of this line relative to those of other approaches should enable a relative ranking. The topology of the covalent link will provide a geometrical approach and thus determine the HB strength efficiency.

4. Intramolecular amide-amide interactions in peptides

4.1. γ-turn models of α-peptides

The γ-turn is the smallest locally folded structure in a diamide model peptide. It has been early recognized as being stabilized by a C7 H-bond that bridges the two ends of the diamide and comes in two variants of opposite folding chirality in α-peptides,[36] the inverse γ-turn, and the direct γ-turn. In these structures, the environments of the C7 H-bond are different, with a side chain in an equatorial or axial position respectively; the HBs are labelled accordingly (C7 eq and C7ax). The inverse γ-turn is usually the most stable, by ca. 2 kcal/mol in the case of the alanine diamide, and is the form usually observed in the gas phase.

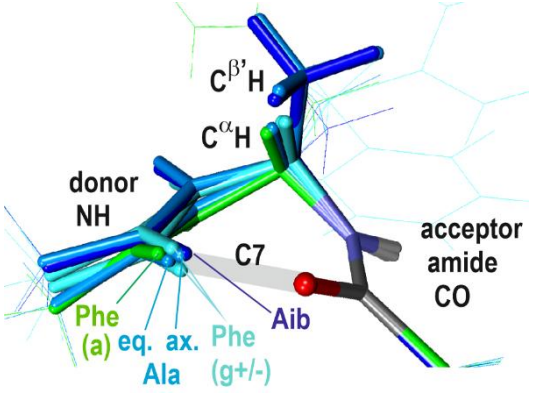


Fig. 6 : Comparative description of the HB approach in γ-turns of the Ala, Phe (*gauche+/-*, *anti*) and Aib series, obtained by superimposing the HB acceptor amides. For the sake of comparison, the Ala C7ax is displayed after a mirror symmetry. Only relevant chemical groups have been highlighted.

a) Assessing the γ-turn approach

The HB strength has been obtained for a whole series of γ-turns in their equilibrium geometries, including Ala (C7eq and C7ax forms), Phe (C7eq with the three possible Phe side chain orientations, i.e., *anti*, *gauche+* and *gauche-*) and the non-proteinogenic amino-isobutyric (Aib) residue (C7, identical to its mirror image). The NBO analysis (see Section 2) carried out on the inverse Ala γ-turn

(C7eq) shows that, despite the delocalization towards the σ^*_{NH} NBO originates from the $n_{O(2)}$ and $n'_{O(2)}$ lone pair NBOs and the $\pi_{CO(2)}$ NBO (see Fig. 3f-h), this turn nevertheless provides a less efficient approach than the N'-side dimer as testified by its position (the lower dark blue diamond in Fig. 5) below that of the magenta N'-dimer line in the ranking scale of Fig. 5. The less favorable approach of the inverse γ-turn compared to this dimer is ascribed to the geometrical constraints imposed by the network of covalent bonds that bridges the amide groups. Figure 5 shows that, along the series of γ-turns assessed, the efficiency varies only slowly, as testified by the slightly curved line, which joins the several γ-turn points. It is nearly parallel to those of the dimers at short HB distances (below 200 pm), with an efficiency comparable to that of the N'-side dimer, but takes a slight negative curvature in the long HB region. This latter feature has to be compared with the changes in the approach geometry along the series, as illustrated by Figure 6 , where the Ala and Phe(*anti*) inverse γ-turns display large geometrical variations (in particular a lesser HB linearity with smaller NH-O angles). In a context where, by comparison with dimers, a certain approach is expected to give rise to a linear dependence in fig. 5, the increasingly negative curvature of the γ-turn line in Fig. 5 can be rationalized as a significant change in the geometric approach of the γ-turn series, at large distances.

b) On the diversity of the equilibrium distances along the γ-turn family

One of the striking points within the γ-turn family is the diversity of the equilibrium distances (and hence HB strengths) encountered along the series, which requires a detailed discussion of the interaction at play in these systems.

The inverse γ-turn: The equilibrium H-bond distance is significantly elongated compared to that of the N-side dimer, in connection with the existence of new constraints, compared to the dimer case, i.e., the interactions responsible for the backbone flexibility.

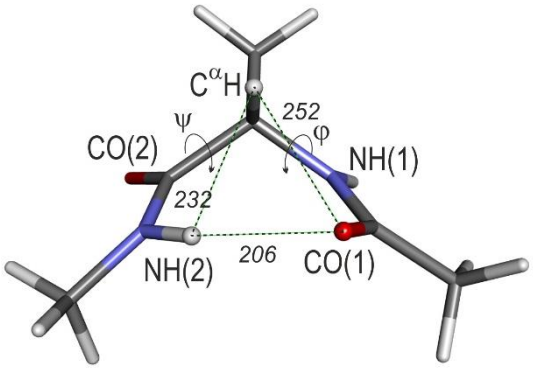


Figure 7: Structure of the inverse γ-turn C7eq conformation of the Ala diamide model, with relevant notations, including the Ramachandran φ, ψ dihedrals. Distances are given in pm.

Beyond the H-bond, the Ala C7eq structure (Figure 7) is also characterized by a C(1)-N(1)-C$^{\alpha}$-C(2) Ramachandran dihedral φ of -82° on the N-terminal side, as well as a short O(1)-H distance (252 pm) in the CO(1)---CαH close contact. As described in detail in Section 2, these features result from i) a strong $n_{N(1)} \rightarrow \sigma^*_{C\alpha C(2)}$ hyperconjugative interaction (Fig. 3c), which favours φ ~ 90° Ramachandran dihedrals, and ii) a significant $\sigma_{C\alpha H} \rightarrow \sigma^*_{NH}$ HC (Fig. 3d) favoring an antiparallel orientation of the vicinal NH and CH bonds (see E(2) values in Table S1). These interactions lead *in fine* to short penalizing O(1)-HC$^{\alpha}$ distances and opposes the HB formation. The molecule also experiences an additional C$^{\alpha}$H---N(2)H contact, with an H-H distance (232 pm), significantly shorter than the distance

reported in crystal survey (238 pm[66]), suggesting a repulsive character of this close contact. In conclusion, the C7eq γ-turn conformation arises from a competition between the C7eq H-bond, on a one hand, and the several interactions which control the backbone flexibility on the other hand, in particular hyperconjugative interactions within the backbone, and to a lesser extent dispersive/close contact interactions involving the H atom of CαH and its closest neighbors (Fig. 7), namely the H atom of the N(2)H bond and the O atom of the carbonyl CO(1).

The inverse γ-turn is also encountered with the phenylalanine (Phe) diamide, with some variability depending upon the orientation of the Phe side chain (Fig. 6 and S2). The two *gauche* orientations exhibit stronger H-bond strengths, with an HB efficiency close to that of the N'-dimer and H-bond distances, significantly shorter than in the Ala γ-turn (Fig. 5). In contrast, the *anti* rotamer of Phe, exhibits a weaker efficiency, together with an increased HB distance. The structures of these species (Figure S2) share the same φ Ramachandran dihedral, which can be rationalized by the existence of the same hyperconjugation interactions and CαH---CO(1) close contacts than with Ala. They differ primarily by the ψ Ramachandran dihedral, which is influenced by interactions between the acceptor CO(2) with the Phe side chain, in particular for the *gauche+* and *anti* rotamers, in which the HB is respectively shortened or elongated.

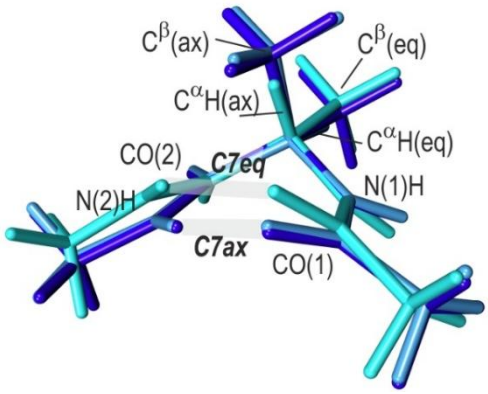


Fig. 8 : Comparison of the C7eq inverse γ- turn of Ala (turquoise), C7ax direct turn of Ala (light blue) and turn of Aib (dark blue) model diamides, obtained by overlaying the N(1), C^{α} and C(2) atoms. For the sake of comparison, the Ala C7ax structure is displayed after a mirror image symmetry. The picture illustrates the change in Ramachandran dihedrals due to the presence of an axial methyl group (C7ax Ala and C7 Aib).

The direct γ-turn : The direct γ-turn is a backbone mirror image of the inverse γ-turn, meaning that the CαH covalent bond and the side chain are now in an equatorial and axial position respectively (Figure 8). However, the corresponding C7ax HB is found to be much stronger (the higher dark blue diamond in Fig. 5), with the φ Ramachandran dihedral adopting a smaller value (72°) compared to the 82° value of the Ala γ-turn mirror image (Fig. 7), which leads to a shorter HB distance (189 pm) together with a larger ψ value (-54°) (Cf. Ala HB distance = 206 pm, and ψ = -75°). This can be rationalized by considering the effect of the side chain methyl group in the axial position upon the HC effects that describe the backbone flexibility (see the HC sets in Table S1). The methyl group does not affect the strong $n_{N(1)} \rightarrow \sigma^*_{C(2)C\alpha}$ HC term (9.6 kcal/mol; HC0 set in Table S1), which tends to favor +90° φ values, but it disrupts the balance between the two other terms of the set in favor of a stronger $n_{N(1)} \rightarrow \sigma^*_{C\alpha C\beta}$ term (5.8 kcal/mol). This latter interaction counterbalances the first term, leading *in fine* to a much smaller φ value (72°) than previously. Interestingly, the presence of the methyl group in axial position also significantly affects HC interactions related to the CαH and CαMe covalent bonds. When comparing the NBO data of C7eq and C7ax Ala systems (Table S1), one

observes: i) a decrease of the HC between the NBO of the σ CαH/CαCβ bond in axial position and the σ*NH(1) acceptor (red data in HC1 set of Table S1) and concomitantly, ii) an increase of the HC stabilization due to the delocalization from the CαCβ/CαH bond in equatorial position to the vicinal CN σ bonds (green data in the HC2 set of Table S1). These changes have two respective consequences: a weakening of the HC, which tended to align the N(1)H bond antiparallel to the CαH/CαCβ(ax) bond, and a strengthening of the interaction, which tends to align the C(2)N(2) and C(1)N(1) σ bonds, antiparallel to the CαCβ/CαH(eq) bond, whose consequences in terms of backbone structure (in particular Ramachandran dihedrals) are illustrated in Figure 8. Consequently, in contrast to the C7eq case, the C7ax system no longer exhibits amide-SC close contacts : the CβH(ax) H atom interacts only weakly with the CO(1) and N(2)H centers, through elongated interaction distances of 257 and 258 pm respectively.

Similar structural effects are encountered in the two (mirror images) γ-turns of the achiral amino-isobutyric acid (Aib), whose Cα atom bears two methyl groups, one equatorial and the other axial with HC features similar to that of the C7ax system (Fig. 6 and 8). Indeed the Aib turn HB is also short (186 pm) and exhibits a larger H-bonding efficiency than the Ala γ-turn, comparable to that of the N'-side dimer (violet diamond in Fig. 5). The NBO analysis shows that the same HC effects at play in the Ala C7ax are also present in Aib (Table S1). The Aib turn HB, however, is still shorter than the Ala C7ax bond, suggesting that an additional factor is also at play. The structural analysis (see Fig. 8) shows that the simultaneous presence of the two side chain methyl groups distorts the Cα sp^3 hybridization and again favors the presence of close contacts, with shortened H-O and H-H distances compared to C7ax: 247 pm in CβH(ax)---CO(1) and 241 pm in CβH(ax)---N(2)H respectively.

Finally, the diversity of the equilibrium distances (and hence HB strengths) along the series can be viewed as the manifestation of the effect of the peptide chain environment on the turn structure. The relatively elongated C7eq HB of the Ala inverse γ-turn, which constitutes a natural HB reference for a γ-turn in peptides and proteins, results from HCs which tend to stiffen the backbone structure, by imposing the φ Ramachandran dihedral and by favouring antiparallel orientations of the vicinal N(1)H and CaH σ bonds. These features are also present in the Phe turns, but the side chain plays here a significant role. The Phe(*anti*) turn, which exhibits the most elongated HBs (Fig. 6), epitomizes an additional frustration due to unfavorable steric effects, namely a Phe SC-backbone close contact. In contrast, in the Phe(*gauche+/-*) turns ancillary SC-backbone interactions allow to compensate for this basic hindrance and eventually enhance the HB. At the top of the series, the C7ax bonds of the Ala direct and Aib turns are much stronger. This is ascribed to the side chain methyl group in axial position, which imposes alternative HC interactions that favour parallel CN amide bonds and *in fine* allow stronger H-bonds to appear. The Aib case is still more constrained due to the simultaneous presence of two bulky side chain methyl groups, which, besides HC effects, also induces additional close contacts.

4.2. Extended β-strand-like forms of α-peptides

Local intraresidue interactions, referred to as C5 interactions, are found in extended β-strand-like conformations of α-peptides (Figs. 1 and 9) and constitute an other iconic approach geometry for two amide groups. Despite the donor amide lies on the C-side of the acceptor, like in the C-side dimer, the fact that donor N(1)H and acceptor CO(2) bonds are facing each other in a quasi-antiparallel disposition because of the strong constrain induced by the small Cα spacer, the non-linear approach is not favorable to H-bonding. The H-bonding nature of the interaction has even been questioned, despite the recent IUPAC broad redefinition of the HB,[67] which qualifies it as a HB.

The C5 HBs of Ala and Phe(*anti*) residues appear quite weak according to the strength scale of Fig. 5 (ΣE_{HB} = 1.1 kcal/mol), i.e., with strengths typically 3 to 4 times weaker than that of a dimer at the same distance, featuring an intrinsically poor HB efficiency of the C5 approach, obviously strongly impaired by the quasi parallel disposition of the donor and the acceptor. As a direct consequence, the main stabilization arises from the $n'_{O(2)}$ NBO (Cf. Fig. 3.f.), which possesses the right *p* character to optimize the overlap with the σ*NH(1) NBO in such an approach. The $\sigma^*_{N(1)H}$ population, at ~ 36 m*e*, exhibits a

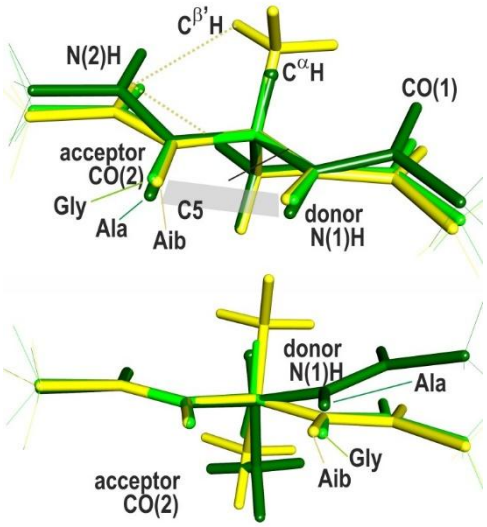


Fig. 9: Comparisons of the C5 extended conformations of Ala (dark green), Gly (green) and Aib (yellow) model diamides. *Top panel*: overlapping the N(1), C^{α} and C(2) atoms provides insights on the differences in Ramachandran dihedrals; *bottom panel*: overlaying the HB acceptor amides illustrates the differences between the HB approaches.

enhancement compared to the ~31-32 m*e* reference for a free amide NH, taken from the HB acceptor *trans*-methylacetamide molecule in the C and N' dimers (see Tables S3 and S4), but remains smaller than that of Ala C7 (~ 43 m*e*). It should be noted that, besides the HB delocalization, the $\sigma^*_{N(1)H}$ NBO also benefits from significant HC interactions from the vicinal $\sigma_{C\alpha H}$ and, to a lesser extent, $\sigma_{C\alpha C\beta}$ NBOs, with E(2) values of 2.6 and 0.6 kcal/mol respectively (Table S1). In this perspective, the spectral shift, usually assigned to the C5 HB interaction,[16] should also be considered as greatly influenced by a substantial HC relative contribution.

Comparison of the Ala C5 structure to its Gly counterpart is interesting since the achiral property of Gly leads to a backbone conformation of Cs symmetry (Figure 9) in contrast to Ala. Examination of the NBO interactions (Table S1) shows that, as in γ-turns, the strong HC interactions which control the Ramachandran φ dihedral angle, i.e., the delocalization from the $n_{N(1)}$ lone pair, is also present in

both Ala and Gly species and occurs towards the $\sigma^*_{C\alpha H}$ and $\sigma^*_{C\alpha H'}$ NBOs for Gly and $\sigma^*_{C\alpha H}$ and $\sigma^*_{C\alpha C\beta}$ NBOs for Ala. In Gly, the HC interactions are the same (9.0 kcal/mol) and lead to φ and ψ Ramachandran dihedrals of 180°; the situation is asymmetric in Ala, where the main delocalization from the $n_{N(1)}$ lone pair goes to the side chain $\sigma^*_{C\alpha C\beta}$ NBO (E(2) value of -9.2 kcal/mol), favoring a situation where the C(1)N(1)$C^{\alpha}C^{\beta}$ dihedral (80°) is closer to 90°, eventually leading to φ = -158° and ψ = 159° Ramachandran dihedrals. This distortion induces a slight increase of the C5 HB distance compared to Gly, which is directly correlated to the changes in stabilization energy (1.1 vs. 1.4 kcal/mol for Ala and Gly resp.; Figure 5).

Another interesting comparison arises from the C5 conformation of the achiral Aib, whose amide network is also planar (Fig. 9). The striking point, however, is the HB enhancement in Aib (ΣE_{HB} = 3.5 kcal/mol) and the shortening of its equilibrium HB distance (Fig. 5). Additionally the proximity of C5 Aib to the dimer lines in the ranking scale of Figure 5, compared to C5 Ala and Gly, features a higher HB efficiency of the C5 approach in Aib. The trend is confirmed when considering squeezed (out-of-equilibrium) conformations of the Ala and Gly C5 structures obtained through full optimization when constraining the HB distance to a series of fixed values (green points in Figure 5). Along this series, the HB strength follows a curved line (green dots) in Fig. 5, mimicking the long distance behavior already observed in the C7 series. Like for this latter geometry, one can notice a significant change in the approach geometry along the C5 series, as depicted in Figure 9, which can account for the negative curvature of the C5 approach line at large HB distances.

The C5 series also shares another feature with the C7 series, i.e., a significant spread of the equilibrium H-distances observed, especially between Ala and Gly residues compared to Aib. A detailed structural analysis shows that in this latter species a repulsive close contact occurs between the acceptor amide N(2)H and the two side chain $C^{\beta'}H$ H atoms (226 pm, see Fig. 9, left panel, much less than the 238 pm value in crystals[66]). It pushes the HB acceptor CO(2) towards the N(1)H donor, leading to a strong HB shortening and enhancement compared to the Ala and Gly residues, where the close contact does not occur. Finally, it should be noted that the Aib molecule presents the same features as diethylglycine, the model molecule chosen by Newberry and Raines[9] to provide evidence for a C5 H-bond in peptides. The present analysis shows that, because of the occurrence of the above mentioned repulsive close contact, the model chosen by these authors grossly overestimates the strength of the C5 HB compared to peptides and proteins.

Besides C5 bonds, other examples of intraresidue HBs can be found in flexible species, such as the C6 HB in extended forms of the Ac-β^3hPhe-NHMe β-peptide[17] (see Fig. 1). The increased flexibility of this backbone ensures a much better efficiency of this C6 approach, compared to C5, closer to that of the weakest C7 γ-turns (Fig.5, ΣE_{HB} indicator ~3.3 kcal/mol with a σ^*_{NH} population of ~ 40 me).

4.3. Intramolecular amide-amide interactions in models of β-turn and 3_{10} helices

β-turns are essential secondary structures, stabilized by C10 HBs, which bridge two amide groups two residues apart, and contain a central amide group.[22] Incipient 3_{10} helices are minimalist helical models, which feature two C10 HBs, one on the C-side terminal and the other on the N-side.[24] They are nearly parallel, similar to those of the β-turns although slightly distorted. Examples of such C10

HB in the gas phase have been taken from experimentally observed β-turns (Ac-Gly-Phe-NHMe, type I and II'),[68] the incipient 3_{10} Ac-Ala-Phe-Ala-NH_2 helix observed experimentally[24] as well as the Ac-$(Ala)_3$-NHMe and Ac-$(Aib)_3$-NHMe model 3_{10} helices. Each helix provides two examples of C10 HB, labelled N-terminal or C-terminal accordingly to their location along the sequence.[24] They slightly differ in geometrical approach and distance because of distortions of the helical structure, either due to the small size of the helix or to the presence of the Phe residue in the sequence.

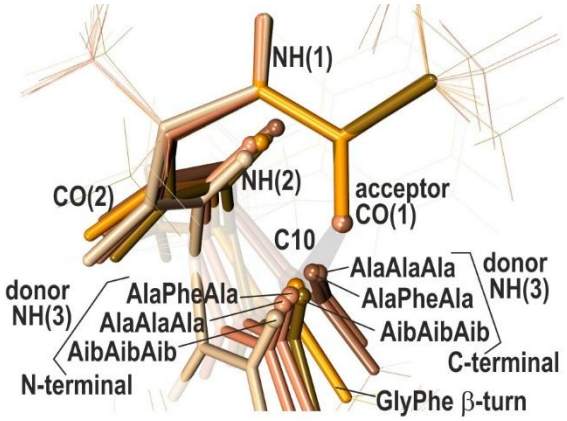


Figure 10: Comparisons of the C10 H-bonds of the type I Ac-Gly-Phe-NHMe β-turn (orange), of the Ac-Ala-Phe-AlaNH_2 and of the Ac-$(Ala)_3$-NHMe and Ac-$(Aib)_3$-NHMe helices (bright and dark brown for the N- and C-terminal sides respectively). For the sake of clarity the side chains are displayed on a line style. The overlay of the HB acceptor amides emphasizes the diversity of HB approaches.

The β-turn HBs exhibit ΣE_{HB} values of the order of ~4 kcal/mol with σ^*_{NH} populations around 42 m*e*. Together with their relatively large HB distance (208 pm), this characterizes them as medium range HBs (Fig. 5), with a modest HB efficiency, as illustrated by the orange eye guide of Fig. 5, passing through the β-turn points, parallel to but lying well below the dimer lines (red and magenta dots). Concerning the helix C10s, a large diversity of HB strengths is observed, ranging from 2 to 5 kcal/mol, with σ^*_{NH} populations between 39 and 47 m*e*., to be correlated with the diversity in terms of geometrical approach within the series (Fig. 10). The N-terminal helix C10s, all lying above the orange line, present a higher efficiency than the β-turn approach, in contrast to the C-terminal C10s, which exhibit a reverse trend. The large diversity in the HB distances within the helix C10 set is ascribed to specific backbone distortions in the helices as noticed earlier and epitomizes the effect of the environment upon the H-bonding through both the control of the HB approach efficiency and the possible HB frustration within the constrained approach.

4.4. Intramolecular amide-amide interactions in di-amide models of β- and γ-peptides

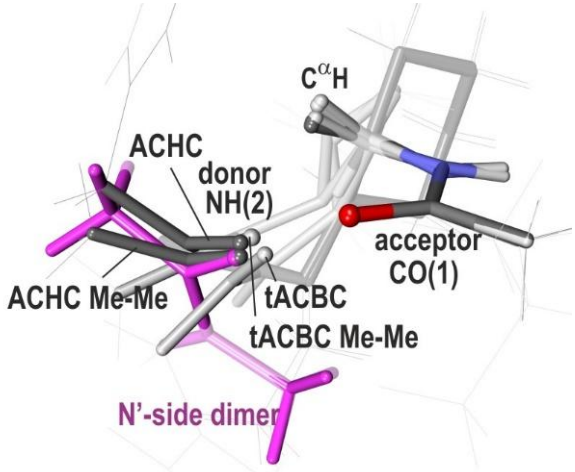


Figure 11: Comparisons of the H-bonds of the tACBC (dark grey; C8 H-bond) and ACHC (grey; C9 H-bond) diamide models with the N'-side dimer of MAA (magenta), which presents a HB approach on the same side of the acceptor. The overlay of the HB acceptor amides emphasizes the differences between the several HB approaches. The tACBC/ACHC acronyms stand for the systems experimentally studied and described in Fig. 1; names followed by Me-Me

stand for model systems with minimalist caps (with acetyl and methylamide groups). For the sake of clarity side chains irrelevant to the discussion are displayed on a line style.

The most stable conformations observed for the ACHC[31] and *t*ACBC[30] backbones are stabilized by C8 and C9 bonds respectively (grey and white disks in Fig. 5), whose efficiencies are found to be as large as that of the C-type dimer. They show $\sum E_{HB}$ and $\sigma^*_{N(1)H}$ population, in the 13-10 kcal/mol and 50-56 m*e* range respectively, comparable to those of C-side dimers at the same HB distance (Fig. 5). These conformations both exhibit the same CαH--- CO(1) close contact than that encountered in the γ-turns of α-peptides, which is caused by the same strong $n_{N(1)} \rightarrow \sigma^*_{C\alpha C\beta}$ and $\sigma_{C\alpha H} \rightarrow \sigma^*_{N(1)H}$ hyperconjugation interactions as in C7eq γ-turns (respective E(2) of 8.2 and 4.6 kcal/mol in ACHC, and 13.5 and 4.3 kcal/mol in tACBC, to be compared with 10.1 and 3.7 kcal/mol in Ala C7eq). However, in contrast to the γ-turns, the additional flexibility, provided by the longer covalent spacers between the amides, together with a favorable range of amide-amide distances, enforced by the cyclic constrain, endows these chains with both an efficient approach and smaller H-bonding distances.

At this stage, one can notice that these species also enable us to document the capacity of apparently ancillary interactions, present in the molecule, in amending the approach and eventually the structure.

In the β-peptide *t*ACBC case, the efficiency is as high as that of the C-side dimer, and the HB distances of these species are very similar, suggesting *a priori* minimal frustrating/enhancing constrains due to the *t*ACBC backbone (grey disk in Fig. 5 at ΣE_{HB} = 9.6 kcal/mol). One should however notice that the bulky caps of this model interact with each other and contribute to the structure. Indeed, a substitution of these caps by smaller methyl groups (tACBC Me Me species) does not affect the HB efficiency (same approach) but decreases the HB distance (grey disk at ΣE_{HB} = 11.1 kcal/mol; tACBC Me Me label in Fig. 5). Being smaller than the bulky caps of *t*-ABCB, the methyl groups do no longer interact with each other, which increases the contribution of backbone intrinsic folding to the H-bonding: the shorter HB distance of the tACBC Me-Me model compared to the dimer illustrates the enhancing role of the β-peptide backbone, in particular due to the *trans*-disposition of the amides on the cyclobutyl ring of this compound.

In contrast, in the experimentally studied ACHC γ-peptide, strong dispersion interactions between the benzyl end and the cyclic side chain tend to make the structure compact with a small HB distance (white disk at ΣE_{HB} = 13.1 kcal/mol in Fig. 5). When substituting the benzyl end by a methyl group in the present calculations, the system adopts a looser structure, with a longer H-bond, a smaller ΣE_{HB} (white disk at ΣE_{HB} = 9.5 kcal/mol; ACHC MeMe label in Fig. 5) as well as a weaker efficiency due to a lesser linearity of the approach (in particular a smaller NH-O angle; see Fig. 11). The efficiency then drops to that of the N'-side dimer, in agreement with the comparable approach in these species as illustrated by Fig. 11. The significantly shorter equilibrium distance compared to the N'-side dimer, however, demonstrates an HB enhancement induced by the constrained γ-peptide backbone.

Interestingly, among all the species studied, only one exhibits a stronger efficiency than the C-side dimer : this is the so-called hydrazino-turn conformation of an Aza β-peptide,[30] whose HB presents a C8+C5 bifurcated nature, due to the presence of a N-heteroatom within the main chain, explaining its apparent extra efficiency (dark grey point above the C-dimer line in Fig. 5). However, in contrast to *t*ACBC, despite this large efficiency, the HB remains relatively modest due to the large H-distance imposed by the rigidity of the hydrazino-turn structure.

Besides these highly efficient HB approaches, the cis-ACBC β-peptide[30] constitutes a dramatic counterexample. The *cis* disposition of the amide about the cyclobutyl ring forces the amides to be relatively close and to adopt nearly stacked conformations, which hampers access to efficient HB approaches. Consequently the most stable conformation is stabilized by a C8 non-linear HB, with a much more modest HB efficiency (similar to those of C10 HBs) and a very elongated HB distance, epitomizing the dramatic effect of the steric constraints in this cyclic backbone.

5. Synthesis: ranking the H-bond approaches and assessing frustrating/enhancing effects on the equilibrium structures

5.1. The approaches

The extended set of conformations considered in the study, with or without covalent linkages between the amide groups, offers various geometrical approaches illustrative of the diversity met in proteins. The ΣE_{HB} - distance semi-log plot derived from NBO analyses (Fig. 5) enables us to rank the corresponding approaches according to their efficiency. The HB strength is found to follow a roughly linear behavior in this plot, as the HB distance varies along a fixed approach. Demonstrated for the dimers, this behavior seems to hold, for each type of secondary structure studied, as long as the geometrical approach does not change significantly along the series considered, as illustrated by γ-turns, β-turn/3-10 helices approaches. The order of the corresponding parallel lines then provides a relative ranking of the approaches, independently from the species that serve to rank them (Cf. vertical arrows in Fig. 5).

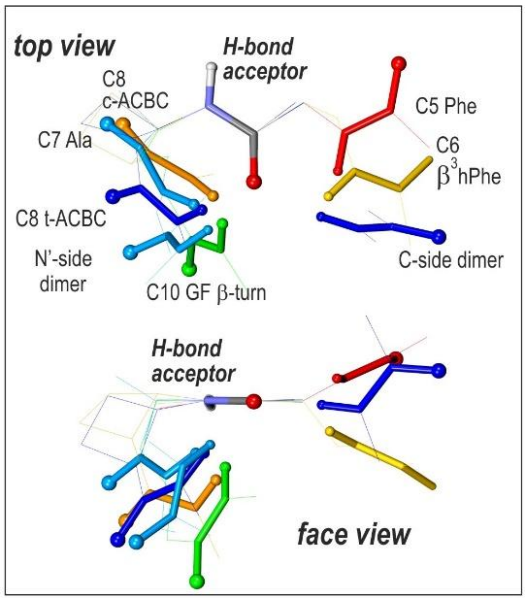


Fig. 12: Various geometrical HB approaches illustrated by selected representative structures studied in the present survey. The HB acceptor amides are overlaid (top: top view for the acceptor amide; bottom: side view), the donor amides are displayed according to a rainbow color code corresponding to increasing HB efficiencies (and not necessary HB strength) when going from red to blue; The amide carbonyl O atom and NH H atom are indicated by large and small balls respectively); for the sake of clarity, the rest of the backbone and side chain have been hidden.

Fig. 12 presents the geometrical approaches corresponding to the several secondary structures and HB types examined, as illustrated by typical representatives. This clearly shows that approaches corresponding to donor NH amides pointing directly towards the O atom of the acceptor carbonyl, i.e. what is often referred to as a linear HB (large NH-O angles), are the most efficient to generate a strong HB : C-side MAA dimer and the C8 of the tACBC residue (Fig. 12, in dark blue). The former corresponds to an alignment of the NH bond, in the carbonyl plane, along one of the carbonyl lone pairs, as anticipated from the usual "rabbit-ears" picturing the lone pairs' electron density.[37, 69] The latter, however, lies clearly off the carbonyl plane and does not fit this simple picture, demonstrating that strong H-bonding approaches can be achieved despite the NH moiety is not pointing directly to the carbonyl lone pairs. In contrast, the N'-side dimer approach is significantly less favorable to H-bonding, in line with a donor NH pointing less directly to the acceptor O atom. With an approach close to the previous ones, γ-turn structures (C7 Ala) exhibit a slightly lesser strength, despite a significant distortion from linearity (Fig. 12, in blue). The β-turn/helical structures, however, only achieve a medium range efficiency, due to the orientation of their donor NH close to the normal of the carbonyl plane, together with a less linear H-bonding geometry (Fig. 12, in green). All the other approaches considered exhibit poor efficiencies, presumably because of the orientation of the donor NH, which tends to be counter-aligned with the carbonyl CO axis, together with a poor linearity (Fig. 12, in yellow orange and red).

The variability observed illustrates, independently from the HB distance, the dependence of the efficiency of the HB approach upon the relative amide-amide orientation allowed by the secondary structure considered, i.e., its backbone arrangement. Apart from the C-side dimer approach, which is essentially defined by the HB itself, the geometry of the other approaches examined is subjected to geometrical constraints imposed by the backbone, such as :

- in γ-turns : a general structural constraint since the two amides share a same Cα. First, the presence of a strong $n_{N(1)} \rightarrow \sigma^*_{C(2)C\alpha}$ HC interaction constrains the φ Ramachandran angle to take a value in the -90° range, which greatly limits the conformational space. Then a second, strong $\sigma_{C\alpha H} \rightarrow \sigma^*_{N(1)H}$ HC interaction constrains the N(1)H bond of the first amide to adopt an orientation antiparallel to the CαH bond in axial position. Both interactions control the local flexibility of the backbone and oppose the establishment of a stronger HB in C7eq structures.

- in β-turns : the architecture of this type of folding, which spans over 2 residues, imposes a structural constrain on the geometrical approach between the extreme amides, which eventually provides HB efficiencies in the medium range, below γ-turns, despite a larger distance between the two Cα atoms (~380 pm) and an increased number of degrees of freedom.

- in the tACBC cyclic β-peptide, the backbone Cα and Cβ atoms are separated by a distance of 258 pm, intermediate between the previous 0 and 380 pm values. The same set of $n_{N(1)} \rightarrow \sigma^*_{C(2)C\alpha}$ and $\sigma_{C\alpha H} \rightarrow \sigma^*_{N(1)H}$ HC interactions as in γ-turns, together with the cyclobutyl ring, provide a scaffolding on the C-terminal side, from which the backbone degrees of freedom on the other side can optimize the H-bonding. It is important to notice that the cyclic feature is a key for the formation of a strong

H-bond, since model calculations have shown that relaxing this constrain leads to the formation of a weaker bond.[30]

- the other constrained structures, in which the approach of the donor NH tends to take an orientation parallel to the CO axis (case of C5, β^3hPhe C6 and cACBC C8 interactions, see Fig. 12), are all strongly penalized from the HB point of view, with low efficiencies.

5.2. The equilibrium structures within a given approach: frustrated vs. enhanced H-bonding

For a molecule, which folds according to a given geometrical H-bonding approach (determined by the secondary structure arrangement, as seen above), the equilibrium conformation adopted, namely the HB distance, is determined by a subtle compromise between H-bonding itself and backbone and side-chain flexibilities, in a broad sense, which *in fine* determines its localization on the line of Fig. 5, which describes the HB approach.

A very flexible backbone is expected to let the set of local H-bonding interactions determine the structure, resulting in an intrinsic distance for the approach considered, similarly to what is happening with the dimers. In contrast, a more rigid backbone can either hamper the formation of an HB of intrinsic strength, leading to a frustrated HB, or, conversely, enhance the HB by forcing donor and acceptor to adopt a short mutual distance. As a result, along the line describing a certain approach in Fig. 5, HBs of equilibrium conformations on the long distance side are frustrated by the backbone, whereas those on the short distance side are enhanced due to the effects of backbone interactions (Cf. oblique arrows in Fig. 5).

At that stage, it is interesting to document, whatever the approach considered, the neutral position, namely the intrinsic distance that would adopt the system in presence of a flexible backbone, whose sole effect nevertheless would be to ensure the approach. In this respect, the models studied in Section 4 provide interesting benchmarks. First, in the dimers, the equilibrium conformation provide the neutral position by definition. Second, the previous analysis of the γ-turn series also suggested to qualify Aib C5 as an enhanced HB (due to the $C^{\beta'}$H-N(2) repulsive close contact ; see Section 4.2) and Ala C7eq as a slightly frustrated (due to intra-backbone HC interactions; section 4.1). Taking these data into account ends up with a neutral region located within a grey shaded area in Fig. 5, arbitrarily enlarged in the bottom to account for the lack of reference in the weak efficiency regions.

The existence of this neutral HB region, then, provides interesting considerations about the frustration/enhancement of the H-bonding in various secondary structures.

α-peptides : The equilibrium structures observed for the several approaches encountered in α-peptides are found to be either in the neutral range or in the frustrated region. The ones, which are the closest to a neutral situation, are the β-turn C10 HBs and some γ-turns. The C5 interactions also appear within the neutral area (Fig. 5), suggesting that the backbone should not oppose strongly to their formation ; however their low position in the strength scale, where the neutral region is ill-defined, makes difficult any clear cut conclusion. In contrast, several helical C10 HBs, on the right hand-side of the grey area, appear frustrated; the Cα-Cα distances in the helical structure being too large for the HB to adopt an optimized HB distance. These observations suggest that in α-peptides

the HB is only one of the components of the structure, stabilizing it, but specific backbone HC features also play a crucial role, in reducing the space of accessible conformations, selecting H-bonding approaches and mediating the HBs strength. Interestingly, the α-peptides conformations showing enhanced HBs are either infrequent secondary structures[70] (direct γ-turns) or even not present in proteins (Aib). Indeed, the C7ax form of Ala is intrinsically less stable than its C7eq inverse γ-turn counterpart, and Aib is not a proteinogenic aminoacid. From a biological perspective, the presence of H atoms on the Cα atoms of aminoacids can be seen as a protection against too strong HBs, which would locally hinder the backbone plasticity, protein folding and probably be damaging to protein function.

Synthetic peptides : The synthetic cyclic β- and γ-peptides studied are capable of achieving high efficiency approaches, comparable to that of the C-type dimer (tACBC, ACHC, Aza-z1), or much lower efficiency approaches (cACBC). Interestingly, the equilibrium structures of the tACBC β-peptides are in, or close to, the neutral HB region, showing that this specific backbone naturally provides a favorable disposition of donor and acceptor amides, *in fine* allowing the formation of HBs of intrinsic strength. Conversely, the cyclically constrained backbone, in addition to the efficiency issue, can also play a significant role in enhancing the HB, compared to the HB strength intrinsic to the approach (ACHC), or in severely frustrating it (cACBC).

6. Assessment of the NH stretch spectral shift as a H-bonding marker in the light of NBO analysis

The NH stretching motion is known for decades as very sensitive to HB strength, and its stretching frequency is often considered, in particular by spectroscopists, as a relevant HB strength marker. The relevance of this approach was recently investigated by Scheiner[71] on the specific example of the water dimer as well as on others types of intermolecular HBs involving different proton acceptor group (carbonyl, carboxylate, imidazole and aromatic ring). Using the sum of the attractive interaction components (electrostatic, induction and dispersion) as a strength reference obtained from a symmetry-adapted perturbation theory (SAPT[72]) partitioning of the total interaction energy, Scheiner showed for the water dimer that, even when squeezing of the complex down to HB distance of 140 pm, the NH stretch red shift remains a monotonically increasing marker. However, this behavior does not necessarily hold for any type of HBs proton acceptor groups, and a detailed analysis of each system is required to conclude. The present benchmark study offers us to address this issue in more complex systems, namely peptides with covalently linked amides, and within a more local framework, the NBO analysis, in which only two-orbital interactions between one NBO donor (a occupied orbital) and one NBO acceptor (a quasi-filled orbital) are taken into account.

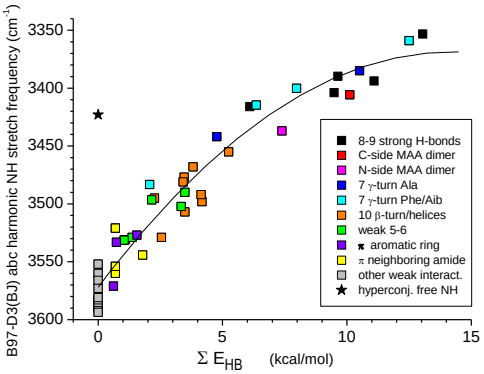


Figure 13 : Dependence of the theoretical (harmonic) NH stretch frequency (B97-D3(BJ)abc /def2-TZVPPD level of theory) with the NBO-based HB strength indicator ΣE_{HB}, with its fit to a quadratic curve, for the amide NH moieties of the model molecules studied (Fig. 1): HB donor NHs (see Table S5), free

NHs (grey and star; see text) and weakly bonded NHs to π aromatic rings (violet) or π amide clouds (yellow).

Figure 13 shows the dependence of the theoretical (harmonic) NH stretch frequency with the NBO-based HB strength indicator, $\sum E_{HB}$, defined from the local assessment of electron delocalisation. The spectral red shift is found to roughly follow the increase of this HB strength indicator, with a slope of ~28 cm^{-1}/(kcal/mol) in the weak HB region (ΣE_{HB} < 5 kcal/mol) and a trend to slowly saturate beyond it. The monotonic dependence obtained indeed qualifies the shift as a satisfactory marker. Beyond this basic minimalist feature required for a marker, one notices that the quality of the frequency predictions nevertheless remains modest: donor amides having the same spectral shift can exhibit stabilization energies differences of the order of 3-6 kcal/mol. Similarly, the average correlation obtained (order 2 polynomial in Fig. 13) yields to an accuracy of the shift prediction of the order of 16 cm^{-1} (RMS error). A striking illustration of this can be found in the spread of the frequency of free NH moieties plotted at $\sum E_{HB}$ = 0 (Fig. 13 ; grey squares) over more than 40 cm^{-1}. Also remarkable is the odd point corresponding to the free NH, vicinal to a N lone pair (hydrazide NH; star in Fig. 13) in the Aza β-peptide compound,[30] which has been interpreted in terms of HC effects involving the donor NBO of a neighboring N atom lone pair.[48] As was already anticipated from the general considerations about hyperconjugative interactions (§ 2.2.2), these latter data also indicate that, besides H-bonding, the spectral shift is significantly affected by specific HC effects, which potentially contribute to generate a noise on the shift-to-$\sum E_{HB}$ correlation of Fig. 13. The average frequency value of 3575 cm^{-1} at the origin of Fig. 13 can be taken as the reference for free amides in peptides, for the present level of theory. Once translated into the experimental scale thanks to the correlation of Figure 2, its provides an averaged experimental frequency reference for free amides of ca. 3500 cm^{-1}.

In an attempt to account for contributions from both H-bonding and intra-backbone hyperconjugative interactions, the spectral shift has also been compared to σ^*_{NH} NBO populations (Fig. 14). Indeed, since the NH stretch spectral shift is primarily sensitive to the length of the NH covalent bond, it is expected to follow any weakening of this bond, as indicated by an increase in the population of the antibonding orbital, whatever the nature of the NBO interaction, either through HB delocalization or HC effects.

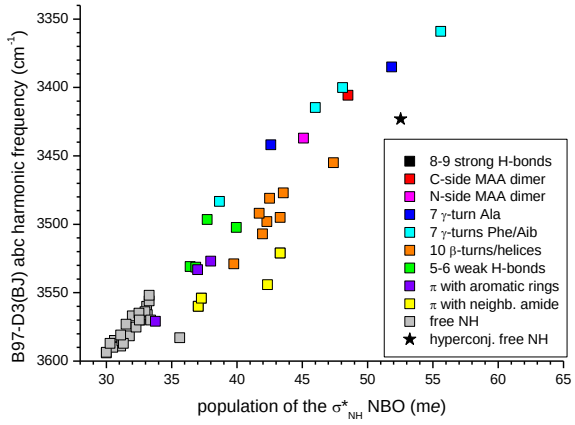


Figure 14 : Dependence of the theoretical (harmonic) NH stretch frequency (B97-D3(BJ)abc /def2-TZVPPD level of theory) upon the σ^*_{NH} NBO population for selected amide NHs in the model molecules studied (Fig. 1): HB donor NHs (see Table S5), free NHs (grey and star; see text) and weakly bonded NHs to π aromatic rings (violet) or π amide clouds (yellow).

Fig. 14 illustrates the trend of the NH stretch red shift to increase with the σ^*_{NH} population. First, the previous odd point assigned to the free hydrazide NH is now found to much better fit to the general trend (star in Fig. 14): it is now accounted for by an important σ^*_{NH} population (53 m*e*), due to the overlap with the vicinal n_N lone pair of the hydrazide nitrogen.[48] A strikingly good correlation between shift and σ^*_{NH} population is also observed in the small shift range (population below 35 m*e*), providing evidence for the dominance of HC interactions upon the spectral shift in this range. They probably remain significant for larger shifts but their relative effect becomes lesser because of an increasing effect of H-bonding. Major deviations from the general trend are nevertheless observed, surprisingly enough owing to the relatively satisfactory shift vs. ΣE_{HB} observed (Fig. 13). These deviations correspond in particular to NHs undergoing close contacts with π clouds of neighboring amides in folded backbones (yellow squares in Figure 14) : the NH of a central amide in a β-turn (main conformation of $AcGlyPheNH_2$)[73] or so-called free NH on the N-terminal side of 3_{10} helices.[74] The NBO analysis confirms a contribution of the lone pair n_N NBO of the neighbor amide (N-terminal side) towards the σ^*_{NH} considered, with E(2) of the order of 0.6-0.8 kcal/mol for all these species, which fairly matches the correlation of Fig. 13. In the same line, the C10 HBs (β-turn and helices; orange squares in Figure 14) also seem to be located below the general trend, despite a correct HB description (Fig. 13, yellow squares). In both cases, the conformations behave as if the σ^*_{NH} population were overestimated. At this stage, one should notice that these NBO σ^*_{NH} populations arise from interactions with different NBO donors, through different types of overlaps. In particular, in β-turns as well as in the N'-side dimer, the major contributor arises from the carbonyl n_O lone pair of mixed *sp* character, in sharp contrast with the γ-turns, the C-side dimer or the tACBC species, where the other n_O lone pair (of p character) is the major contributor to ΣE_{HB} (distribution of the several contributions to ΣE_{HB} are given in the Supp. Info.). In this regard, the free hydrazide NH, evoked above, even represents an extreme example, since the type of overlap is also different : the n_N NBO of hydrazide overlaps the N-side external lobe of the σ^*_{NH} NBO, whereas in HBs the donor NBOs overlap the σ^*_{NH} NBO on its opposite, H-side, external lobe. These observations suggest that NBO σ^*_{NH} populations arising from different origins (types of donors, of overlaps, etc…) behave as if they had various efficiencies in terms of NH stretch red shift, which might point out a limitation of the NBO analysis.

Finally, despite the fact that the NH stretch spectral shift depends on both H-bonding and hyperconjugative effects, the natural NBO-based indicator, which would globally account for these two effects, namely the σ^*_{NH} population, does not provide a satisfactory correlation. Instead, the NBO-based theoretical HB-indicator ΣE_{HB} chosen in the present work (Fig. 13) exhibits a much better behavior, despite not accounting for hyperconjugative interactions. These latter being more modest, their eventual effects is a slight blurring of the NH stretch vs. ΣE_{HB} correlation. If care is taken to avoid species with strong HC effects (such as in hydrazides), the NH spectral shift can thus been considered as a fair marker of the HB, with a monotonic behavior even for strong HBs, with HB distances as short as 180 pm.

7. Conclusion

The present Natural Bond Orbital analysis of electron delocalization in a series of isolated capped peptides enables us to rationalize the diversity of HB strengths and spectral shifts in conformations observed experimentally by laser spectroscopists and beyond. It emphasizes both the role of the relative orientation of the donor and acceptor amides, i.e., the geometrical approach, and of specific structural and flexibility features of the peptide backbone/environment, in controlling respectively the efficiency of the approach and the HB equilibrium distance of the conformations considered. The study demonstrates that HB in capped peptides, and thus in protein chains, are most of the time constrained, and, depending on the effects mentioned above, they can be either frustrated or, conversely, enhanced.

The NBO analysis turns out to be a tool of choice, shedding light on both the HB-related electron delocalization and backbone-induced hyperconjugative effects, inasmuch as both effects are found to influence the NH-stretch spectral shift, i.e., the main measureable quantity on which most of the spectroscopic approaches are based.

Conflicts of interest

There are no conflicts of interest to declare

Acknowledgements

Support from the French National Research Agency (ANR) is acknowledged (Grant ANR-17-CE29-0008 "TUNIFOLD-S"). This work was granted access to the HPC facility of [TGCC/CINES/IDRIS] under the Grant 2019- A0050807540 awarded by GENCI (Grand Equipement National de Calcul Intensif) and to the CCRT High Performance Computing (HPC) facility at CEA under the Grant CCRT2019-p606bren.

References

1. Pace, C. N.; Scholtz, J. M.; Grimsley, G. R., Forces stabilizing proteins. *FEBS Lett.* **2014,** *588* (14), 2177-2184.
2. Dill, K. A.; MacCallum, J. L., The Protein-Folding Problem, 50 Years On. *Science* **2012,** *338* (6110), 1042-1046.
3. Eisenberg, D., The discovery of the α-helix and β-sheet, the principal structural features of proteins. *Proc. Natl. Acad. Sci. U. S. A.* **2003,** *100* (20), 11207-11210.
4. Donohue, J., Hydrogen bonded helical configurations of the polypeptide chain *Proc. Natl. Acad. Sci. U. S. A.* **1953,** *39* (6), 470-478.
5. Bolen, D. W.; Rose, G. D., Structure and energetics of the hydrogen-bonded backbone in protein folding. *Annu. Rev. Biochem.* **2008,** *77*, 339-362.
6. Rose, G. D.; Fleming, P. J.; Banavar, J. R.; Maritan, A., A backbone-based theory of protein folding. *Proc. Natl. Acad. Sci. U. S. A.* **2006,** *103* (45), 16623-16633.
7. Rose, G. D.; Gierasch, L. M.; Smith, J. A., Turns in peptides and proteins. *Adv.Protein Chem.* **1985,** *37*, 1-109.
8. Milner-White, E. J.; Ross, B. M.; Ismail, R.; Belhadjmostefa, K.; Poet, R., One type of γ-turn rather than the other gives rise to chain reversal in proteins. *J. Mol. Biol.* **1988,** *204* (3), 777-782.
9. Newberry, R. W.; Raines, R. T., A prevalent intraresidue hydrogen bond stabilizes proteins. *Nat. Chem. Biol.* **2016,** *12* (12), 1084.

10. Gloaguen, E.; Mons, M., Isolated neutral peptides. *Topics in current chemistry* **2015,** *364*, 225-70.
11. Schwing, K.; Gerhards, M., Investigations on isolated peptides by combined IR/UV spectroscopy in a molecular beam - structure, aggregation, solvation and molecular recognition. *Int. Rev. Phys. Chem.* **2016,** *35* (4), 569-677.
12. Rijs, A. M.; Oomens, J., IR Spectroscopic Techniques to Study Isolated Biomolecules. In *Gas-Phase Ir Spectroscopy and Structure of Biological Molecules*, Rijs, A. M.; Oomens, J., Eds. Springer-Verlag Berlin: Berlin, 2015; Vol. 364, pp 1-42.
13. Dian, B. C.; Longarte, A.; Mercier, S.; Evans, D. A.; Wales, D. J.; Zwier, T. S., The infrared and ultraviolet spectra of single conformations of methyl-capped dipeptides: N-acetyl tryptophan amide and N-acetyl tryptophan methyl amide. *J. Chem. Phys.* **2002,** *117* (23), 10688-10702.
14. Chin, W.; Mons, M.; Dognon, J. P.; Piuzzi, F.; Tardivel, B.; Dimicoli, I., Competition between local conformational preferences and secondary structures in gas-phase model tripeptides as revealed by laser spectroscopy and theoretical chemistry. *Phys. Chem. Chem. Phys.* **2004,** *6* (10), 2700-2709.
15. Gerhards, M., Spectroscopy of Neutral Peptides In The Gas Phase: Structure, Reactivity, Microsolvation and Molecular Recognition. In *Principles of Mass Spectrometry Applied to Biomolecules*, Laskin, J.; Lifshitz, C., Eds. Wiley & Sons: Hoboken, NJ, 2006; pp 3-62.
16. Chin, W.; Piuzzi, F.; Dimicoli, I.; Mons, M., Probing the competition between secondary structures and local preferences in gas phase isolated peptide backbones. *Phys. Chem. Chem. Phys.* **2006,** *8* (9), 1033-1048.
17. Baquero, E. E.; James, W. H.; Choi, S. H.; Gellman, S. H.; Zwier, T. S., Single-conformation ultraviolet and infrared spectroscopy of model synthetic foldamers: β-peptides Ac-β^3-hPhe-NHMe and Ac-β^3-hTyr-NHMe. *J. Am. Chem. Soc.* **2008,** *130* (14), 4784-4794.
18. Baquero, E. E.; James, W. H.; Choi, S. H.; Gellman, S. H.; Zwier, T. S., Single-conformation ultraviolet and infrared spectroscopy of model synthetic foldamers: β-peptides Ac-β^3-hPhe-β^3-hAla-NHMe and Ac-β^3-hAla-β^3-hPhe-NHMe. *J. Am. Chem. Soc.* **2008,** *130* (14), 4795-4807.
19. Buchanan, E. G.; James, W. H.; Choi, S. H.; Guo, L.; Gellman, S. H.; Muller, C. W.; Zwier, T. S., Single-conformation infrared spectra of model peptides in the amide I and amide II regions: Experiment-based determination of local mode frequencies and inter-mode coupling. *J. Chem. Phys.* **2012,** *137* (9), 094301.
20. Gerhards, M.; Unterberg, C.; Gerlach, A.; Jansen, A., β-sheet model systems in the gas phase: Structures and vibrations of Ac-Phe-NHMe and its dimer $(Ac\text{-}Phe\text{-}NHMe)_2$. *Phys. Chem. Chem. Phys.* **2004,** *6* (10), 2682-2690.
21. Chin, W.; Dognon, J. P.; Canuel, C.; Piuzzi, F.; Dimicoli, I.; Mons, M.; Compagnon, I.; von Helden, G.; Meijer, G., Secondary structures of short peptide chains in the gas phase: Double resonance spectroscopy of protected dipeptides. *J. Chem. Phys.* **2005,** *122* (5), 8.
22. Chin, W.; Dognon, J. P.; Piuzzi, F.; Tardivel, B.; Dimicoli, I.; Mons, M., Intrinsic folding of small peptide chains: Spectroscopic evidence for the formation of β-turns in the gas phase. *J. Am. Chem. Soc.* **2005,** *127* (2), 707-712.
23. Chin, W.; Piuzzi, F.; Dognon, J. P.; Dimicoli, I.; Mons, M., Gas-phase models of γ-turns: Effect of side-chain/backbone interactions investigated by IR/UV spectroscopy and quantum chemistry. *J. Chem. Phys.* **2005,** *123* (8), 11.
24. Chin, W.; Piuzzi, F.; Dognon, J. P.; Dimicoli, L.; Tardivel, B.; Mons, M., Gas phase formation of a 3(10)-helix in a three-residue peptide chain: Role of side chain-backbone interactions as evidenced by IR-UV double resonance experiments. *J. Am. Chem. Soc.* **2005,** *127* (34), 11900-11901.
25. Brenner, V.; Piuzzi, F.; Dimicoli, I.; Tardivel, B.; Mons, M., Spectroscopic evidence for the formation of helical structures in gas-phase short peptide chains. *J. Phys. Chem. A* **2007,** *111* (31), 7347-7354.

26. Fricke, H.; Funk, A.; Schrader, T.; Gerhards, M., Investigation of secondary structure elements by IR/UV double resonance spectroscopy: Analysis of an isolated β-sheet model system. *J. Am. Chem. Soc.* **2008,** *130* (14), 4692-4698.
27. Biswal, H. S.; Loquais, Y.; Tardivel, B.; Gloaguen, E.; Mons, M., Isolated Monohydrates of a Model Peptide Chain: Effect of a First Water Molecule on the Secondary Structure of a Capped Phenylalanine. *J. Am. Chem. Soc.* **2011,** *133* (11), 3931-3942.
28. Stamm, A.; Bernhard, D.; Gerhards, M., Structural investigations on a linear isolated depsipeptide: the importance of dispersion interactions. *Phys. Chem. Chem. Phys.* **2016,** *18* (22), 15327-15336.
29. Gloaguen, E.; Pagliarulo, F.; Brenner, V.; Chin, W.; Piuzzi, F.; Tardivel, B.; Mons, M., Intramolecular recognition in a jet-cooled short peptide chain: γ-turn helicity probed by a neighbouring residue. *Phys. Chem. Chem. Phys.* **2007,** *9* (32), 4491-4497.
30. Alauddin, M.; Gloaguen, E.; Brenner, V.; Tardivel, B.; Mons, M.; Zehnacker-Rentien, A.; Declerck, V.; Aitken, D. J., Intrinsic Folding Proclivities in Cyclic -Peptide Building Blocks: Configuration and Heteroatom Effects Analyzed by Conformer-Selective Spectroscopy and Quantum Chemistry. *Chemistry-a European Journal* **2015,** *21* (46), 16479-16493.
31. Walsh, P. S.; Kusaka, R.; Buchanan, E. G.; James, W. H.; Fisher, B. F.; Gellman, S. H.; Zwier, T. S., Cyclic Constraints on Conformational Flexibility in gamma-Peptides: Conformation Specific IR and UV Spectroscopy. *J. Phys. Chem. A* **2013,** *117* (47), 12350-12362.
32. Blodgett, K. N.; Zhu, X.; Walsh, P. S.; Sun, D. W.; Lee, J.; Choi, S. H.; Zwier, T. S., Conformer-Specific and Diastereomer-Specific Spectroscopy of α β α Synthetic Foldamers: Ac-Ala-β(ACHC)-Ala-NHBn. *J. Phys. Chem. A* **2018,** *122* (14), 3697-3710.
33. Allen, F. H.; Bird, C. M.; Rowland, R. S.; Raithby, P. R., Resonance-induced hydrogen bonding at sulfur acceptors in R1R2C=C and R1CS2- systems. *Acta Crystallogr. Sect. B-Struct. Commun.* **1997,** *53*, 680-695.
34. Perczel, A.; Angyan, J. G.; Kajtar, M.; Viviani, W.; Rivail, J. L.; Marcoccia, J. F.; Csizmadia, I. G., Peptide models.1. Topology of selected peptide conformational potential-energy surfaces (Glycine and Alanine derivatives). *J. Am. Chem. Soc.* **1991,** *113* (16), 6256-6265.
35. Endredi, G.; Perczel, A.; Farkas, O.; McAllister, M. A.; Csonka, G. I.; Ladik, J.; Csizmadia, I. G., Peptide models .15. The effect of basis set size increase and electron correlation on selected minima of the ab initio 2D-Ramachandran map of For-Gly-NH_2 and For-L-Ala-NH_2. *Theochem-J. Mol. Struct.* **1997,** *391* (1-2), 15-26.
36. Vargas, R.; Garza, J.; Hay, B. P.; Dixon, D. A., Conformational study of the alanine dipeptide at the MP2 and DFT levels. *J. Phys. Chem. A* **2002,** *106* (13), 3213-3218.
37. Adhikari, U.; Scheiner, S., Preferred Configurations of Peptide-Peptide Interactions. *J. Phys. Chem. A* **2013,** *117* (2), 489-496.
38. DiStasio, R. A.; Gobre, V. V.; Tkatchenko, A., Many-body van der Waals interactions in molecules and condensed matter. *J. Phys.-Condes. Matter* **2014,** *26* (21), 16.
39. Gloaguen, E.; de Courcy, B.; Piquemal, J. P.; Pilme, J.; Parisel, O.; Pollet, R.; Biswal, H. S.; Piuzzi, F.; Tardivel, B.; Broquier, M.; Mons, M., Gas-Phase Folding of a Two-Residue Model Peptide Chain: On the Importance of an Interplay between Experiment and Theory. *J. Am. Chem. Soc.* **2010,** *132* (34), 11860-11863.
40. Joseph, J.; Jemmis, E. D., Red-, blue-, or no-shift in hydrogen bonds: A unified explanation. *J. Am. Chem. Soc.* **2007,** *129* (15), 4620-4632.
41. Albrecht, M.; Rice, C. A.; Suhm, M. A., Elementary peptide motifs in the gas phase: FTIR aggregation study of formamide, acetamide, N-methylformamide, and N-methylacetamide. *J. Phys. Chem. A* **2008,** *112* (33), 7530-7542.
42. Forsting, T.; Gottschalk, H. C.; Hartwig, B.; Mons, M.; Suhm, M. A., Correcting the record: the dimers and trimers of trans-N-methylacetamide. *Phys. Chem. Chem. Phys.* **2017,** *19* (17), 10727-10737.
43. Stone, A. J., Computation of charge-transfer energies by perturbation-theory. *Chem. Phys. Lett.* **1993,** *211* (1), 101-109.

44. Stone, A. J.; Szalewicz, K., Reply to "Comment on 'Natural Bond Orbitals and the Nature of the Hydrogen Bond"'. *J. Phys. Chem. A* **2018,** *122* (2), 733-736.
45. Alabugin, I. V.; Gilmore, K. M.; Peterson, P. W., Hyperconjugation. *Wiley Interdiscip. Rev.-Comput. Mol. Sci.* **2011,** *1* (1), 109-141.
46. Alabugin, I. V.; dos Pasos Gomes, G.; Abdo, M. A., Hyperconjugation. *Wiley Interdiscip. Rev.-Comput. Mol. Sci.* **2019,** *9*, e1389.
47. Bohlmann, F., Zur Konfigurationsbestimmung von Chinolizin-Derivaten. *Angew. Chem.-Int. Edit.* **1957,** *69* (20), 641-642.
48. Gloaguen, E.; Brenner, V.; Alauddin, M.; Tardivel, B.; Mons, M.; Zehnacker-Rentien, A.; Declerck, V.; Aitken, D. J., Direct Spectroscopic Evidence of Hyperconjugation Unveils the Conformational Landscape of Hydrazides. *Angew. Chem.-Int. Edit.* **2014,** *53* (50), 13756-13759.
49. Glendening, E. D.; Landis, C. R.; Weinhold, F., Natural bond orbital methods. *Wiley Interdiscip. Rev.-Comput. Mol. Sci.* **2012,** *2* (1), 1-42.
50. Reed, A. E.; Curtiss, L. A.; Weinhold, F., Intermolecular interactions from a natura bond orbital, donor-acceptor viewpoint. *Chem. Rev.* **1988,** *88* (6), 899-926.
51. Weinhold, F., Natural bond orbital analysis: A critical overview of relationships to alternative bonding perspectives. *J. Comput. Chem.* **2012,** *33* (30), 2363-2379.
52. Biswal, H. S.; Wategaonkar, S., Nature of the N-H - - - S Hydrogen Bond. *J. Phys. Chem. A* **2009,** *113* (46), 12763-12773.
53. James, W. H.; Buchanan, E. G.; Muller, C. W.; Dean, J. C.; Kosenkov, D.; Slipchenko, L. V.; Guo, L.; Reidenbach, A. G.; Gellman, S. H.; Zwier, T. S., Evolution of Amide Stacking in Larger gamma-Peptides: Triamide H-Bonded Cycles. *J. Phys. Chem. A* **2011,** *115* (47), 13783-13798.
54. Nakhaei, E.; Nowroozi, A.; Ravari, F., The influence of 5-fluorouracil anticancer drug on the DNA base pairs; a quantum chemical study. *J. Biomol. Struct. Dyn.* **2019,** *37* (1), 1-19.
55. Pal, T. K.; Sankararamakrishnan, R., Quantum Chemical Investigations on Intraresidue Carbonyl-Carbonyl Contacts in Aspartates of High-Resolution Protein Structures. *J. Phys. Chem. B* **2010,** *114* (2), 1038-1049.
56. Scheiner, S., Extrapolation to the complete basis set limit for binding energies of noncovalent interactions. *Comput. Theor. Chem.* **2012,** *998*, 9-13.
57. Vogt, N.; Savelyev, D. S.; Giricheva, N. I.; Islyaikin, M. K.; Girichev, G. V., Accurate Determination of Equilibrium Structure of 3-Aminophthalonitrile by Gas Electron Diffraction and Coupled-Cluster Computations: Structural Effects Due to Intramolecular Charge Transfer. *J. Phys. Chem. A* **2016,** *120* (44), 8853-8861.
58. Puzzarini, C.; Biczysko, M.; Barone, V.; Largo, L.; Pena, I.; Cabezas, C.; Alonso, J. L., Accurate Characterization of the Peptide Linkage in the Gas Phase: A Joint Quantum-Chemical and Rotational Spectroscopy Study of the Glycine Dipeptide Analogue. *Journal of Physical Chemistry Letters* **2014,** *5* (3), 534-540.
59. Cabezas, C.; Varela, M.; Cortijo, V.; Jimenez, A. I.; Pena, I.; Daly, A. M.; Lopez, J. C.; Cativiela, C.; Alonso, J. L., The alanine model dipeptide Ac-Ala-NH_2 exists as a mixture of C-7(eq) and C-5 conformers. *Phys. Chem. Chem. Phys.* **2013,** *15* (7), 2580-2585.
60. Grimme, S.; Ehrlich, S.; Goerigk, L., Effect of the Damping Function in Dispersion Corrected Density Functional Theory. *J. Comput. Chem.* **2011,** *32* (7), 1456-1465.
61. Rappoport, D.; Furche, F., Property-optimized Gaussian basis sets for molecular response calculations. *J. Chem. Phys.* **2010,** *133* (13), 11.
62. Schafer, A.; Huber, C.; Ahlrichs, R., Fully optimized contracted gaussian-basis sets of triple zeta valence quality for atoms Li to Kr. *J. Chem. Phys.* **1994,** *100* (8), 5829-5835.
63. *TURBOMOLE V7.2 2017, a development of University of Karlsruhe and Forschungszentrum Karlsruhe GmbH, 1989-2007, TURBOMOLE GmbH, since 2007; available from http://www.turbomole.com*. , 2017.
64. Glendening, E. D.; Reed, A. E.; Carpenter, J. E.; Weinhold, F. *NBO (Version 3.1)* 2009.
65. Frisch, M. J.; Trucks, G. W.; Schlegel, H. B.; Scuseria, G. E.; Robb, M. A.; Cheeseman, J. R.; Scalmani, G.; Barone, V.; Petersson, G. A.; Nakatsuji, H.; Li, X.; Caricato, M.; Marenich, A. V.;

Bloino, J.; Janesko, B. G.; R. Gomperts, R.; B. Mennucci, B.; Hratchian, H. P.; Ortiz, J. V.; Izmaylov, A. F.; Sonnenberg, J. L.; Williams-Young, D.; Ding, F.; Lipparini, F.; Egidi, F.; Goings, J.; Peng, B.; Petrone, A.; Henderson, T.; Ranasinghe, D.; Zakrzewski, V. G.; Gao, J.; Rega, N.; Zheng, G.; Liang, W.; Hada, M.; Ehara, M.; Toyota, K.; Fukuda, R.; Hasegawa, J.; Ishida, M.; Nakajima, T.; Honda, Y.; Kitao, O.; Nakai, N.; Vreven, T.; Throssell, K.; Montgomery, J., J. A. ; Peralta, J. E.; F. Ogliaro, F.; M. J. Bearpark, M. J.; J. J. Heyd, J. J.; Brothers, E. N.; Kudin, K. N.; Staroverov, V. N.; Keith, T. A.; Kobayashi, R.; Normand, J.; Raghavachari, K.; Rendell, A. P.; Burant, J. C.; Iyengar, S. S.; Tomasi, J.; Cossi, M.; Millam, J. M.; Klene, M.; Adamo, C.; Cammi, R.; Ochterski, J. W.; Martin, R. L.; Morokuma, K.; Farkas, O.; Foresman, J. B.; Fox, D. J. Gaussian 16, Revision A.03; Gaussian, Inc., Wallingford CT.: 2016.

66. Rowland, R. S.; Taylor, R., Intermolecular nonbonded contact distances in organic crystal structures: Comparison with distances expected from van der Waals radii. *Journal of Physical Chemistry* **1996,** *100* (18), 7384-7391.

67. Arunan, E.; Desiraju, G. R.; Klein, R. A.; Sadlej, J.; Scheiner, S.; Alkorta, I.; Clary, D. C.; Crabtree, R. H.; Dannenberg, J. J.; Hobza, P.; Kjaergaard, H. G.; Legon, A. C.; Mennucci, B.; Nesbitt, D. J., Definition of the hydrogen bond (IUPAC Recommendations 2011). *Pure and Applied Chemistry* **2011,** *83* (8), 1637-1641.

68. Loquais, Y.; Gloaguen, E.; Habka, S.; Vaquero-Vara, V.; Brenner, V.; Tardivel, B.; Mons, M., Secondary Structures in Phe-Containing Isolated Dipeptide Chains: Laser Spectroscopy vs Quantum Chemistry. *J. Phys. Chem. A* **2015,** *119* (23), 5932-5941.

69. Wiberg, K. B.; Marquez, M.; Castejon, H., Lone pairs in carbonyl-compounds and ethers. *Journal of Organic Chemistry* **1994,** *59* (22), 6817-6822.

70. Guruprasad, K.; Rajkumar, S., β- and γ-turns in proteins revisited: A new set of amino acid turn-type dependent positional preferences and potentials. *J. Biosci.* **2000,** *25* (2), 143-156.

71. Scheiner, S., Interpretation of Spectroscopic Markers of Hydrogen Bonds. *ChemPhysChem* **2016,** *17* (14), 2263-2271.

72. Rybak, S.; Jeziorski, B.; Szalewicz, K., Many-body symmetry-adapted perturbation-theory of intermolecular interactions - H_2O and HF dimers. *J. Chem. Phys.* **1991,** *95* (9), 6576-6601.

73. Chaudret, R.; de Courcy, B.; Contreras-García, J.; Gloaguen, E.; Zehnacker-Rentien, A.; Mons, M.; Piquemal, J.-P., Unraveling Non Covalent Interactions within Flexible Biomolecules: from electron density topology to gas phase spectroscopy. *Physical Chemistry Chemical Physics* **2014,** *16* (6), 2285-2288.

74. Chin, W.; Piuzzi, F.; Dognon, J.-P.; Dimicoli, I.; Tardivel, B.; Mons, M., Gas phase formation of a 3_{10}-helix in a three-residue peptide chain: Role of side chain-backbone interactions as evidenced by IR-UV double resonance experiments. *J. Am. Chem. Soc.* **2005,** *127* (34), 11900-11901.